Kinematics of filaments and cores associated with regions of high-mass star formation

Lev Pirogov (Institute of Applied Physics, Nizhny Novgorod, Russia)

International Conference
Submillimeter and Millimeter Astronomy: Objectives and Instruments

AstroSpaceCenter, Moscow
12—16 April 2021

Kinematics of the S242 & Mon R1 filaments

Turbulence in S242 and other regions

Kinematics of the L1287 core from fitting model molecular line maps into observed ones

Herschel (2009-2013)

Orion A

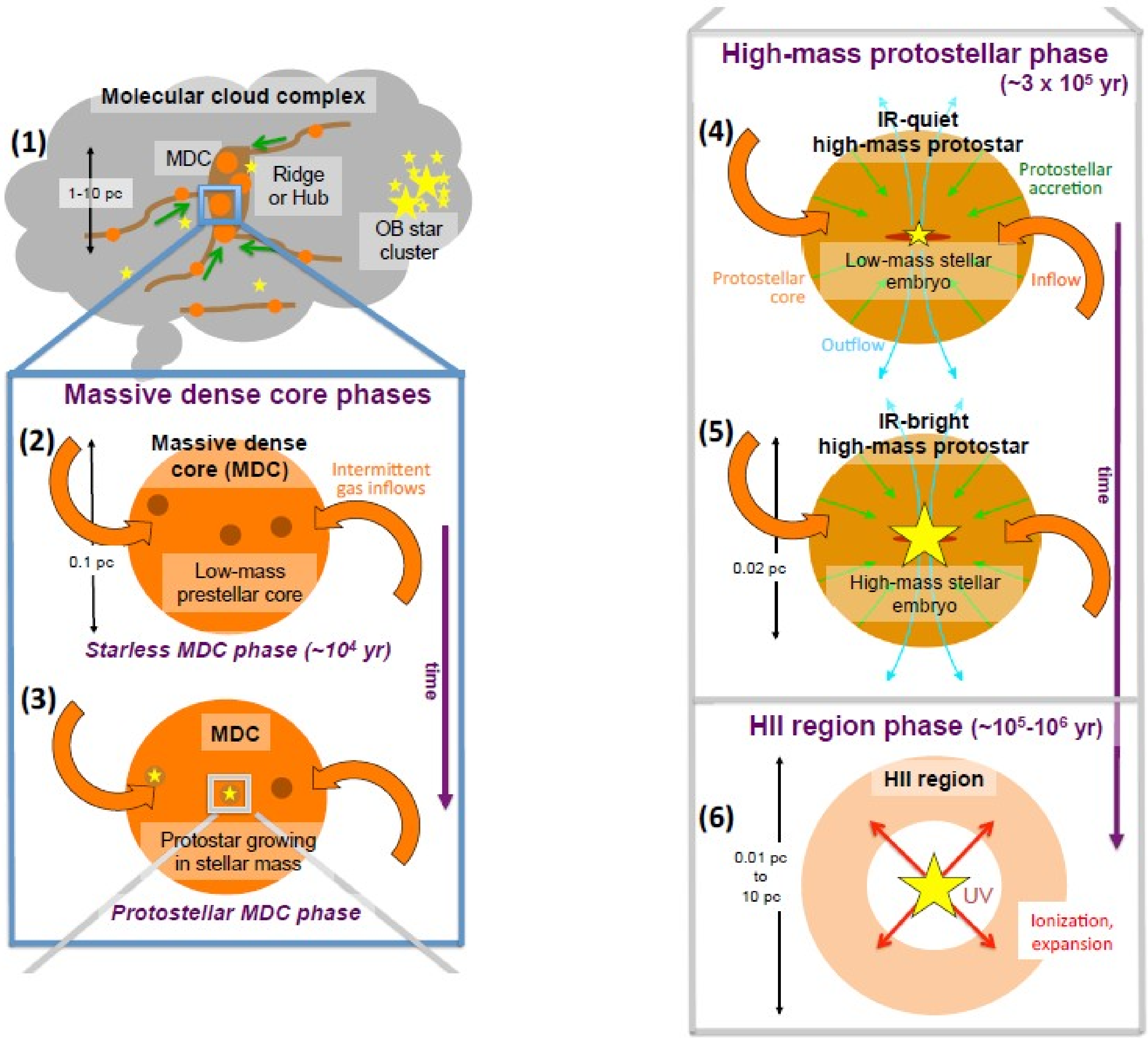

Tige et al. 2017
Andre et al. 2018

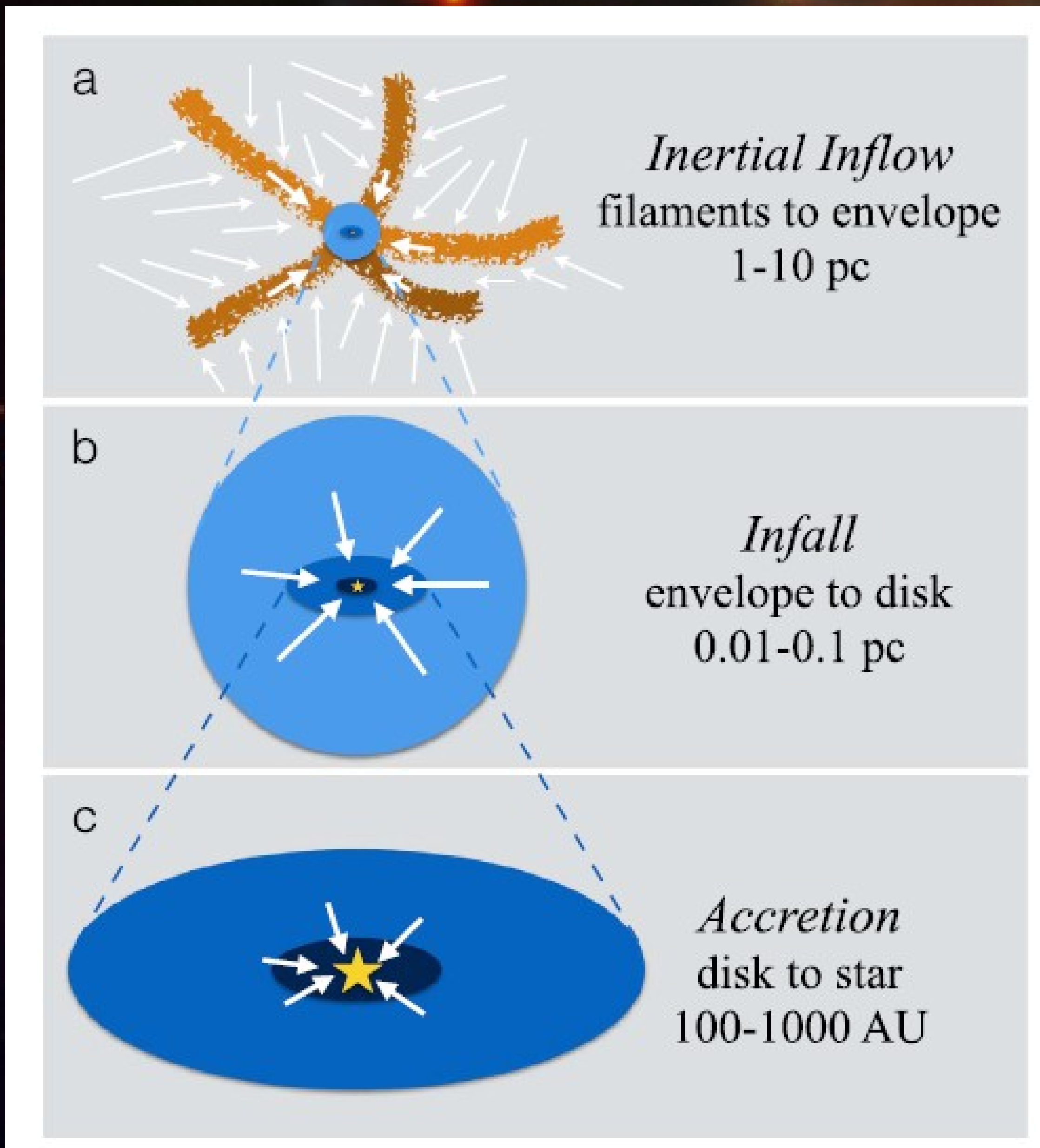

Padoan et al. 2020

IRAM-30m

Onsala-20m

NRO-45m

Kinematics of the S242 & Mon R1 filaments

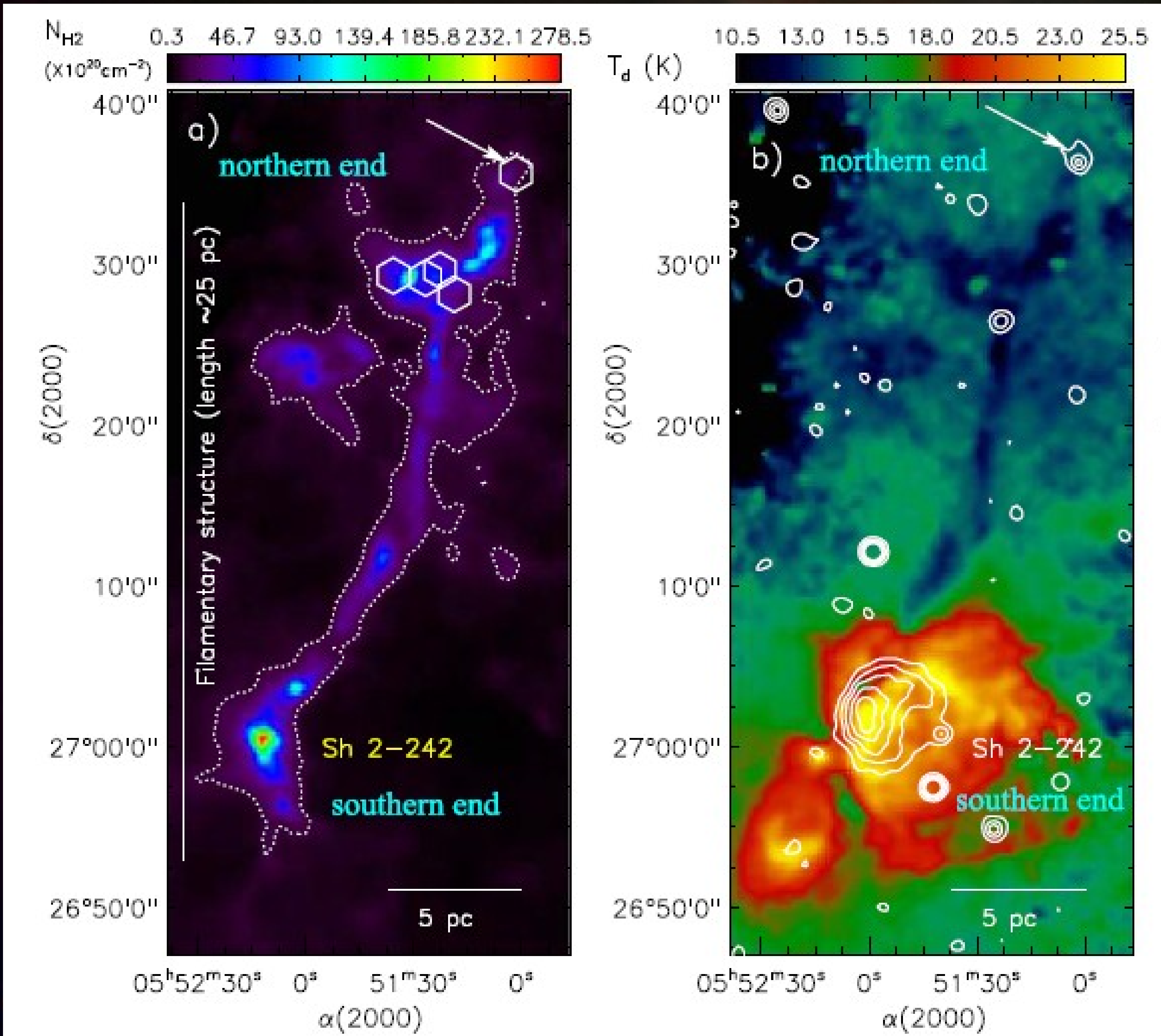

The S242 filament

Column density and dust temperature maps

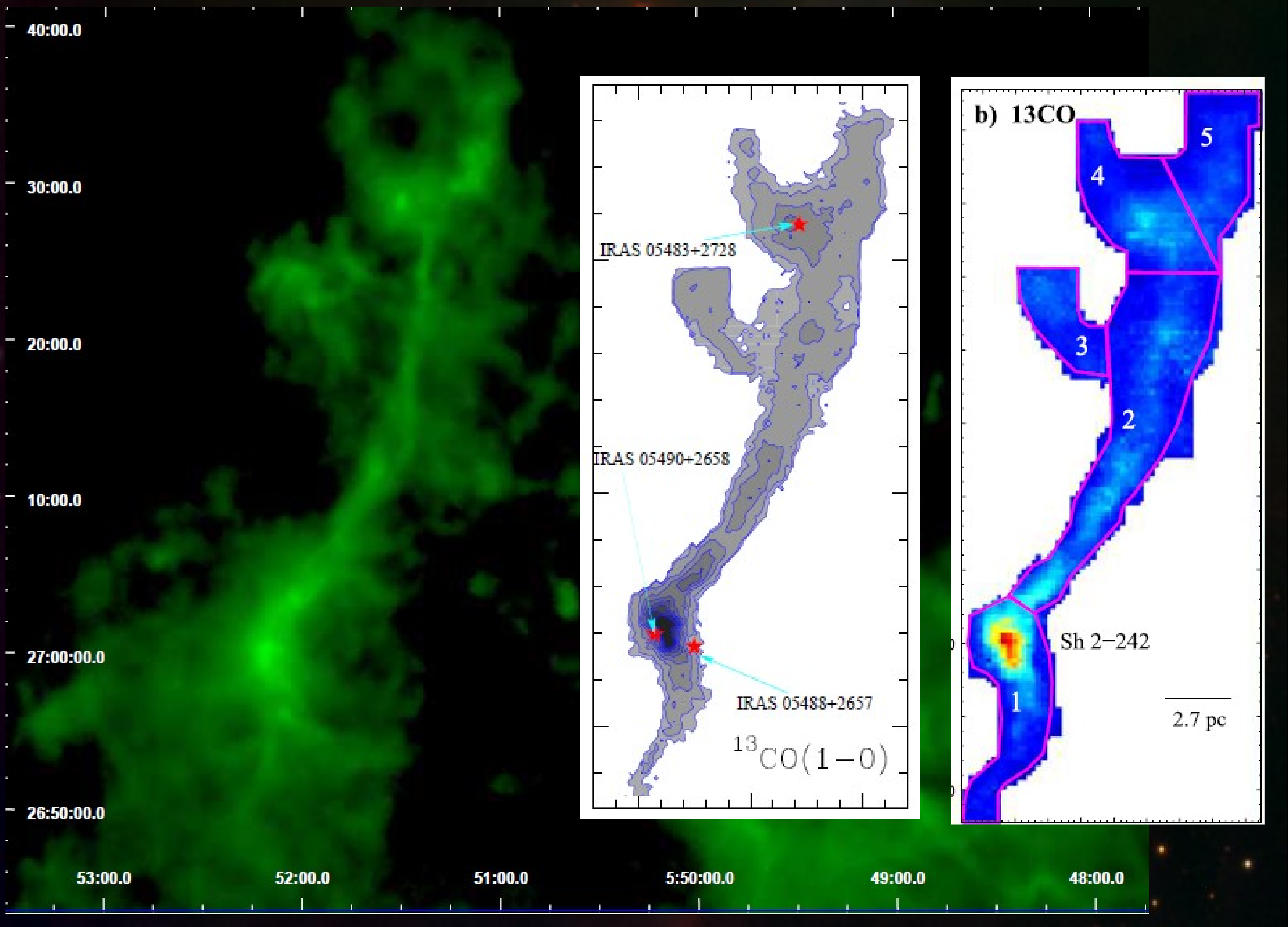
40:00.0
30:00.0
20:00.0
10:00.0
27:00:00.0
26:50:00.0
53:00.0
52:00.0
51:00.0
5:50:00.0
49:00.0
48:00.0
IRAS 05483+2728
IRAS 05490+2658
IRAS 05488+2657
$^{13}CO(1-0)$
b) 13CO
1
2
3
4
5
Sh 2−242
2.7 pc

Position-velocity diagrams

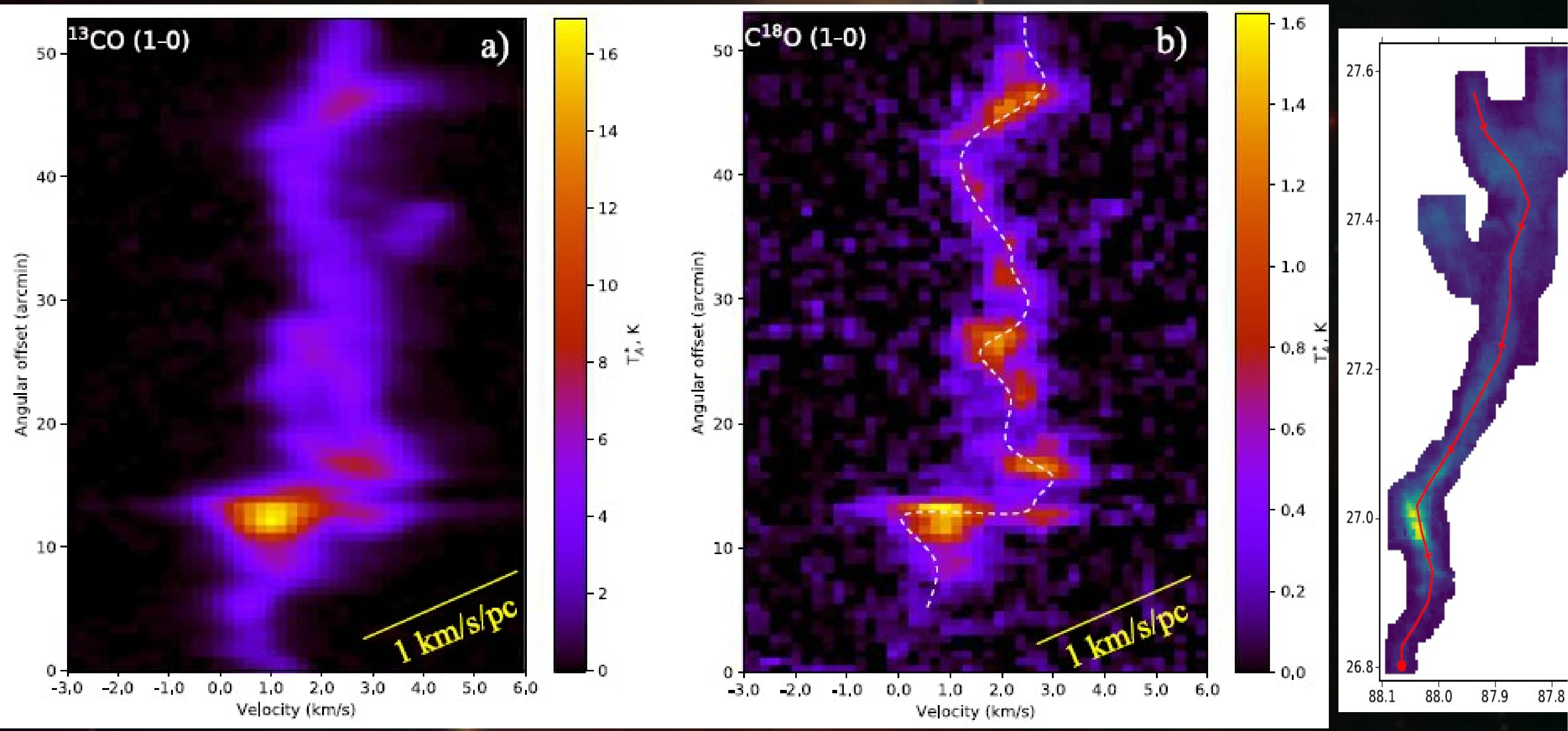

(Dewangan, Pirogov, Ryabukhina et al. 2019)

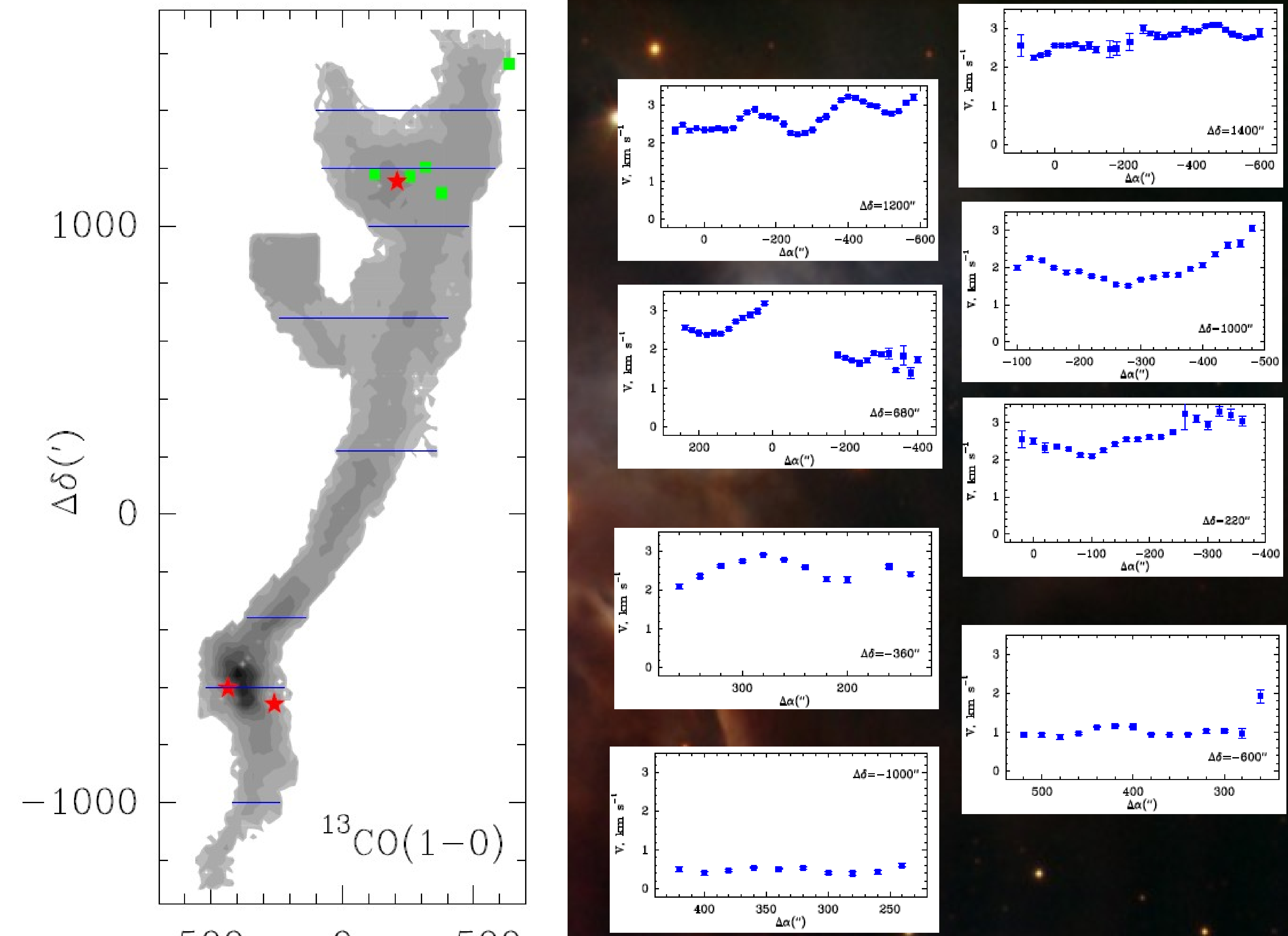

Velocity across the filament

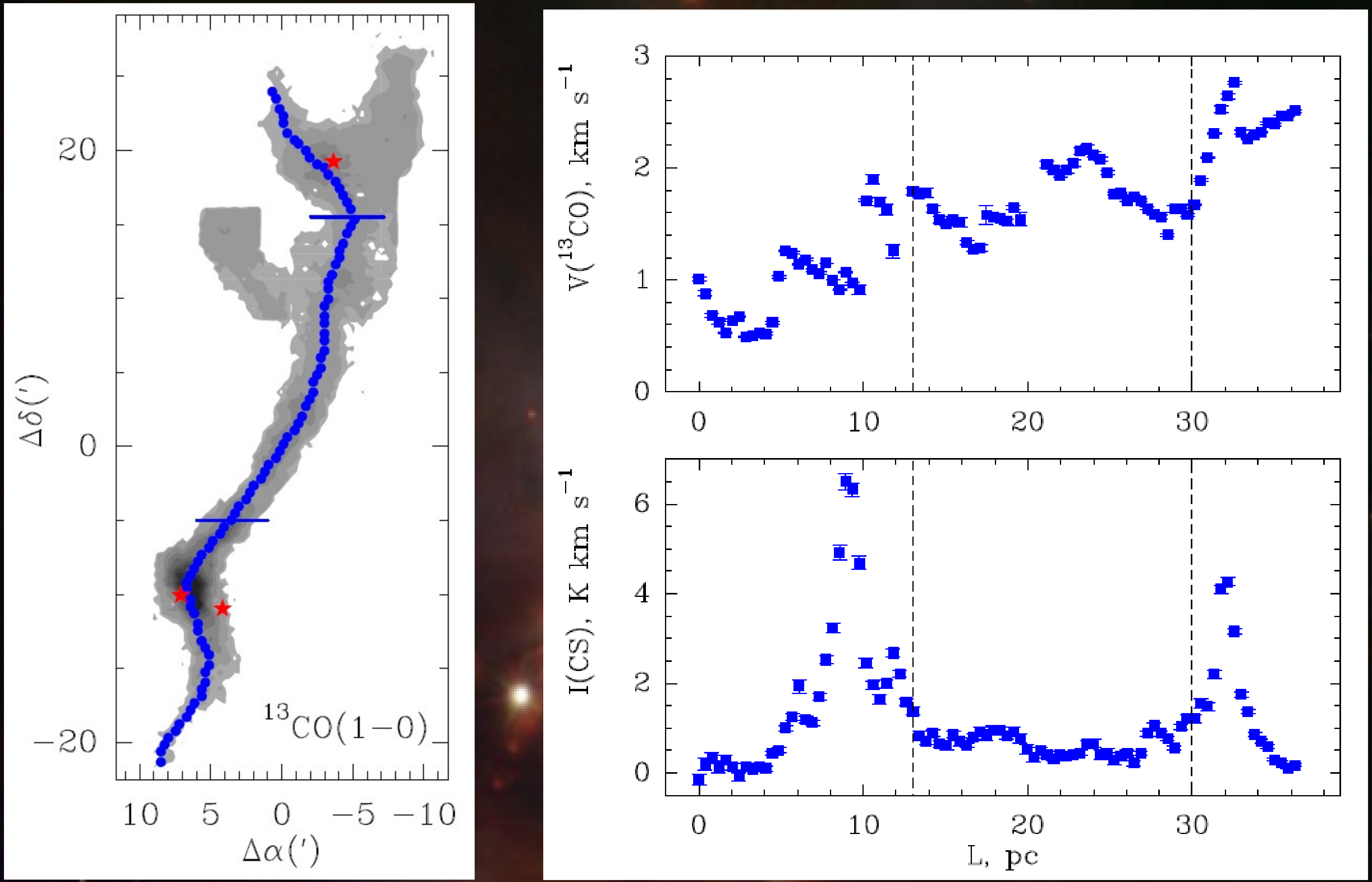

V(13CO) and I(CS) versus the distance along the filament

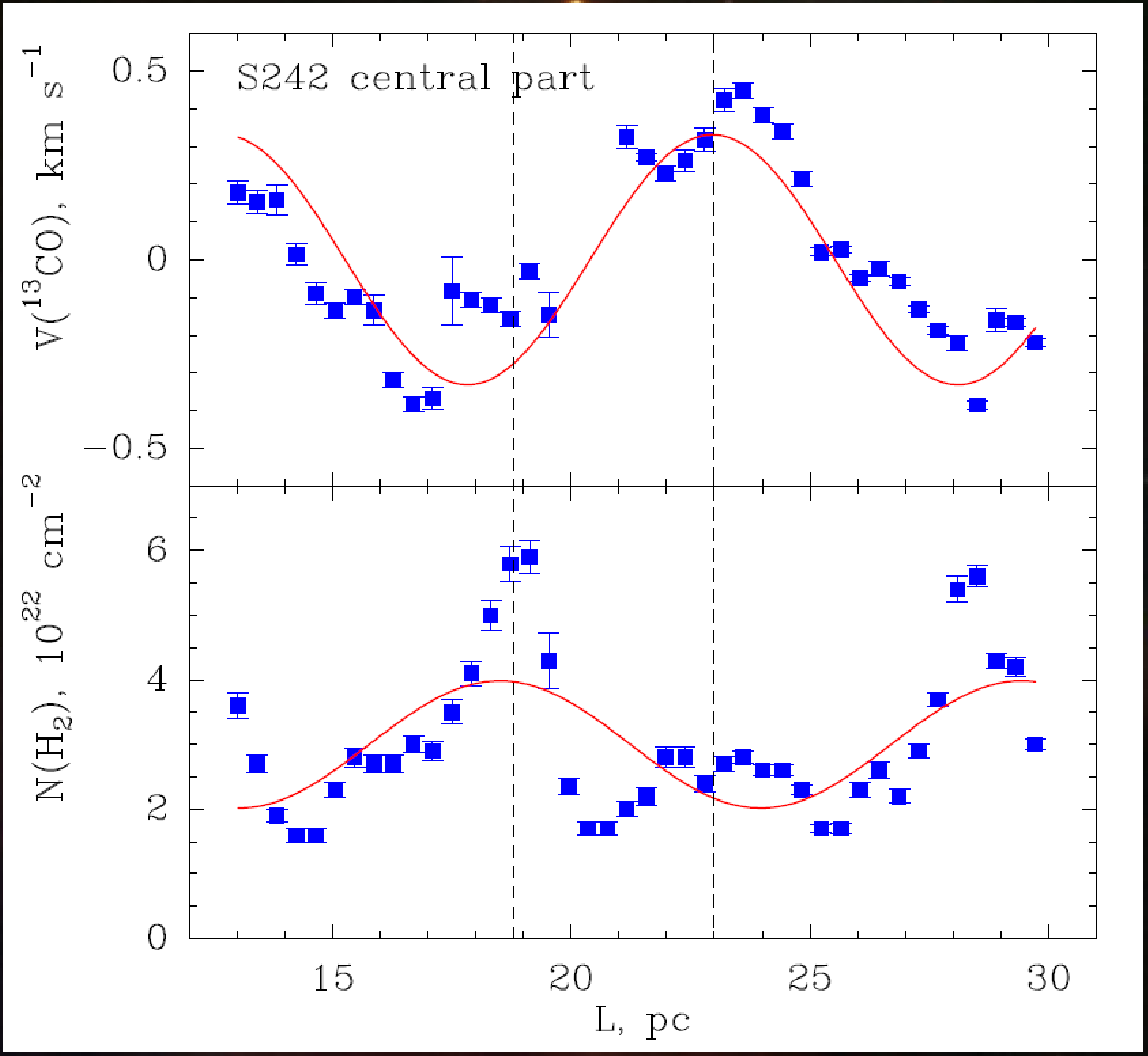

V(13CO) velocity and H2 column density profiles for the central part of the S242 filament.

λ(V), λ(N) ~ 10.5 pc

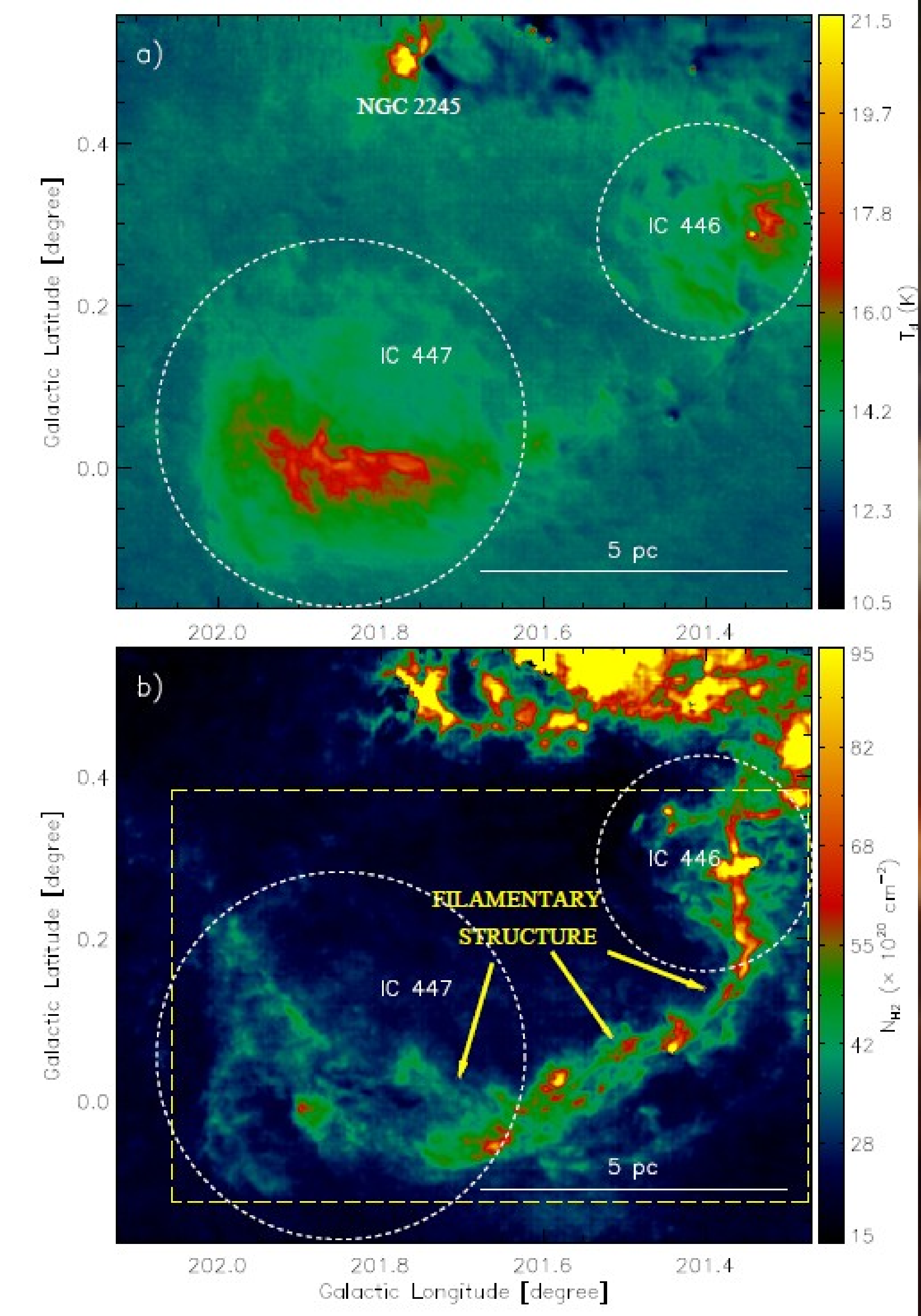

The Mon R1 filament

Dust temperature and column density maps

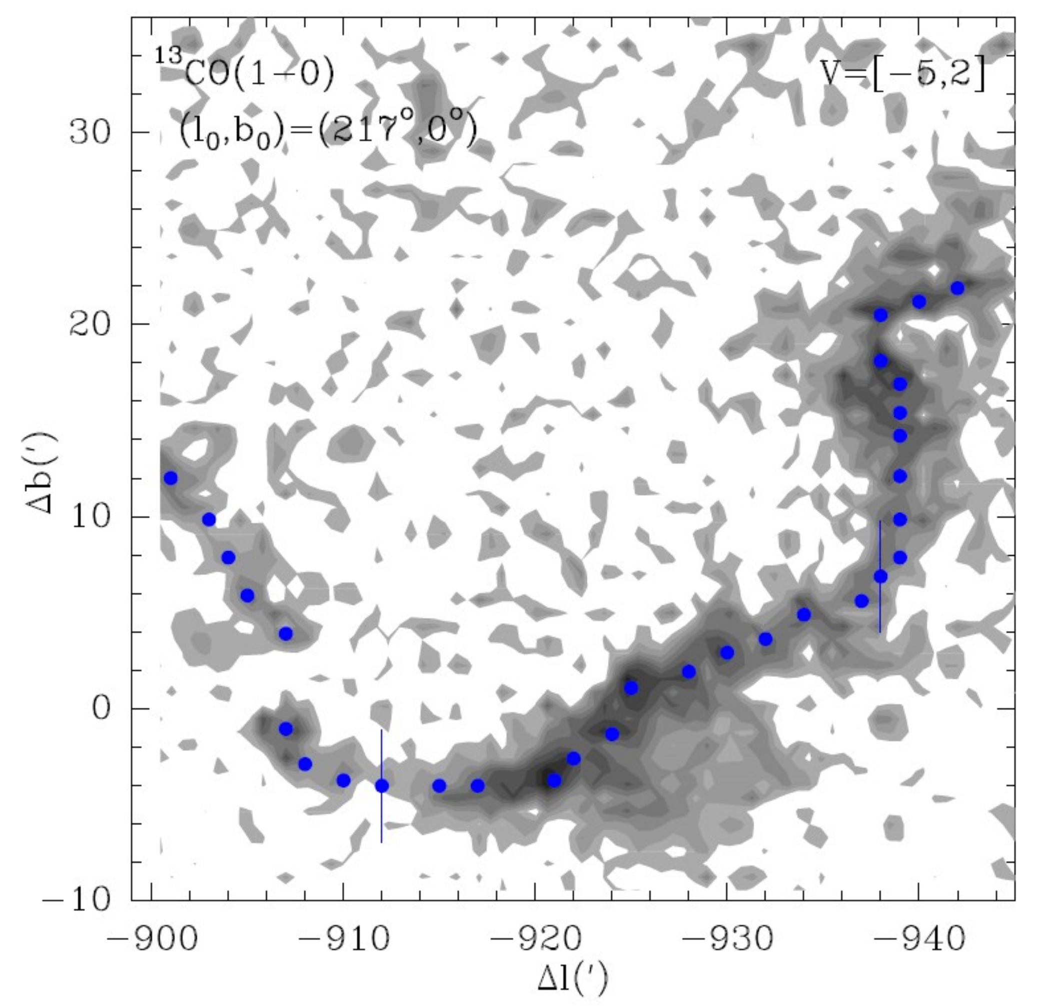

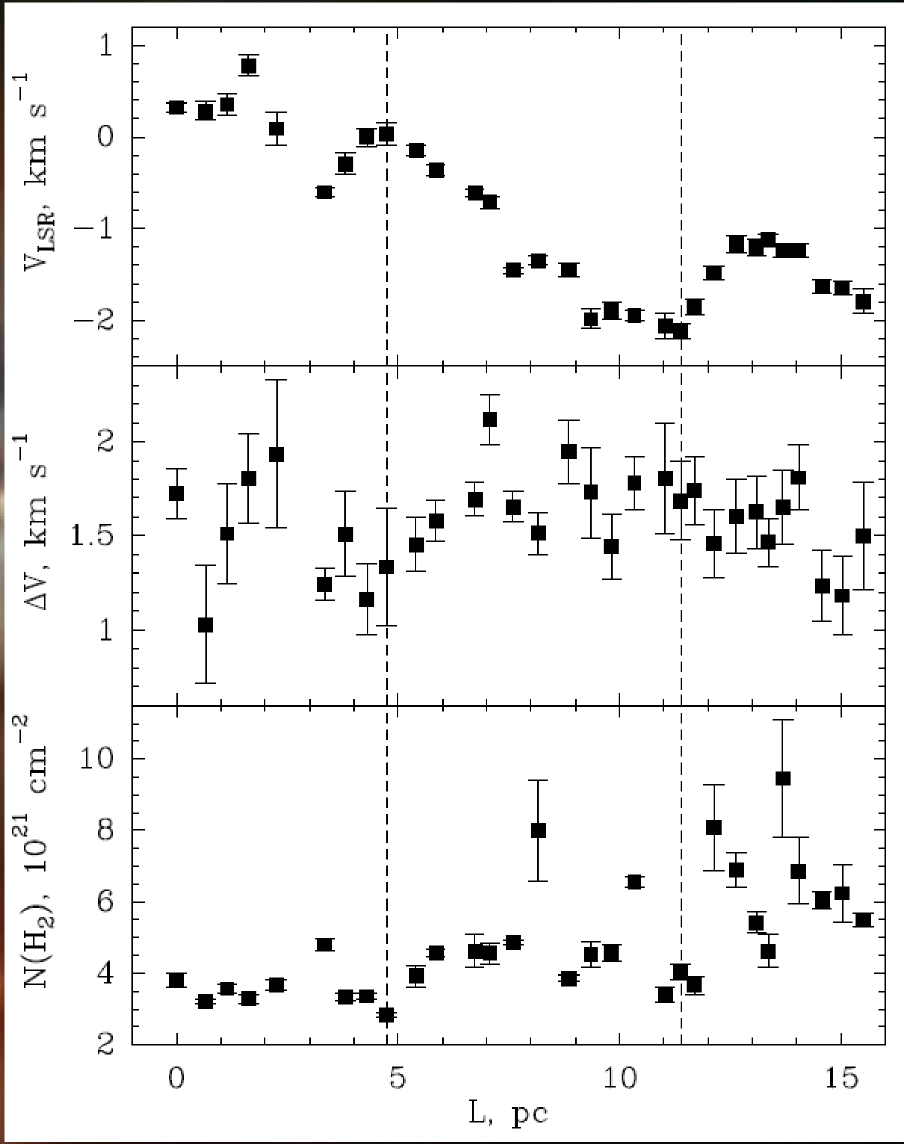

V(13CO), ΔV(13CO) and column density along the Mon R1 filament.

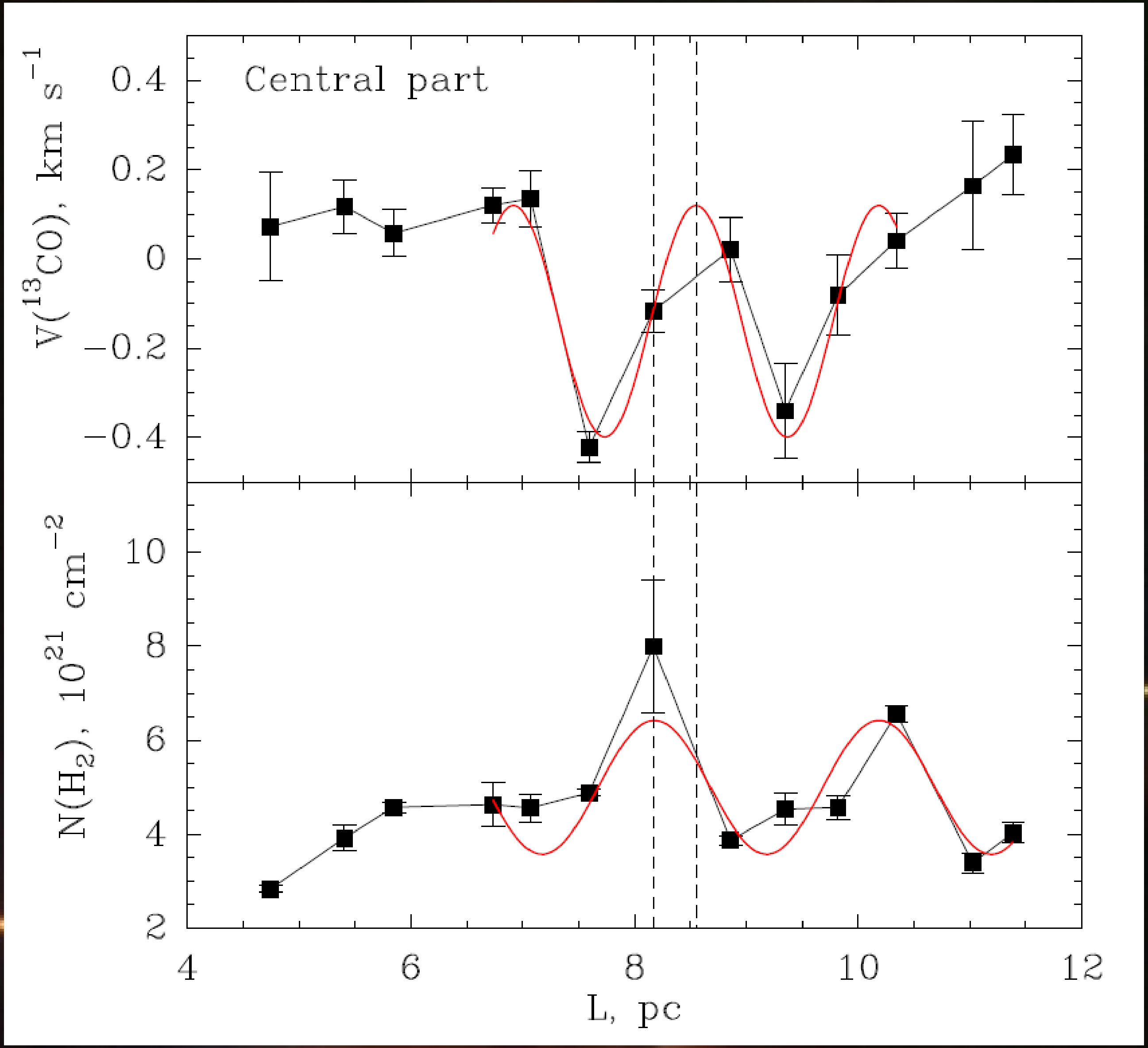

Velocity (with linear gradient subtracted) and column density for the central part of the Mon R1 filament.
$\lambda(V) \sim 1.6$ pc, $\lambda(N) \sim 2$ pc.

Fragmentation in the cylinder of infinite length

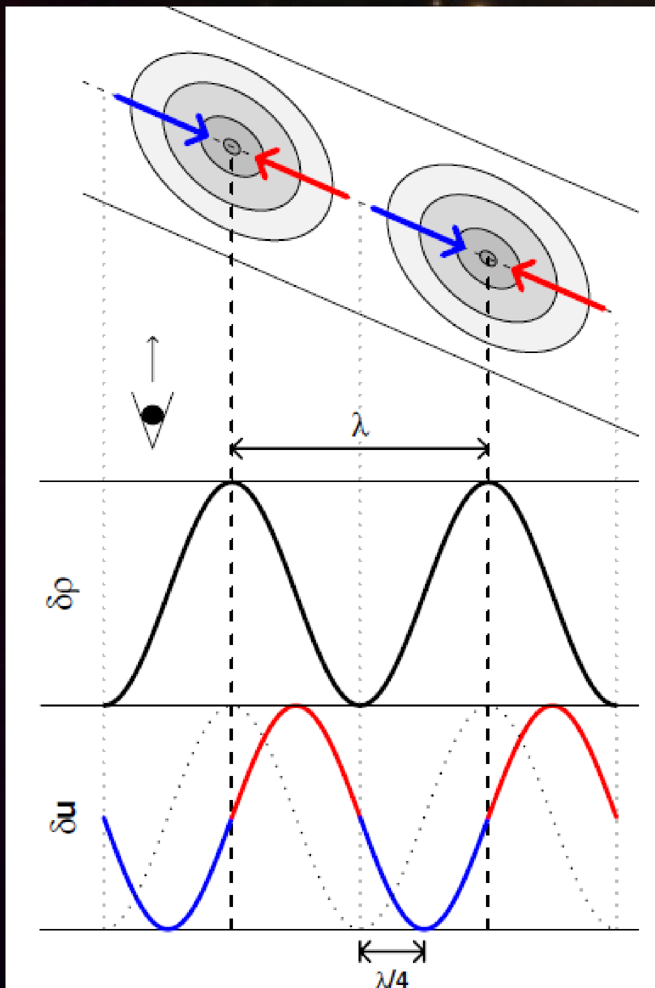

Stodólkiewicz, J. S. 1963, Acta Astron., 13, 30

Ostriker, J. 1964, ApJ, 140, 1056

Hacar, A., & Tafalla, M. 2011, A&A, 533, 34

$$n(r) = \frac{n_\circ}{(1 + (r/H)^2)^{2}},$$

$$\lambda_\mathrm{f} = 3.94H,$$

	H (pc)	λ (pc)	$\Delta\lambda$ (pc)
Mon R1	~ 1	~ 1.6 (V)	~ 0.4
S242	~ 2.5	~ 10.5	~ 4
L1517 (Hacar & Tafalla)	~ 0.1	~ 0.2	~ 0.05

Condition $\lambda \geq 3.94$ H is not valid for Mon R1 and L1517

Condition $\Delta\lambda = \lambda/4$ is not valid for S242

S242 and Mon R1are the filaments with massive star-forming sites located at their ends.

Velocity profiles along the filaments have both global gradients and oscillatory patterns.
There are also local velocity gradients close the ends of filaments probably due to gas accelaration towards star-forming sites.

There are velocity and column density oscillations in the filaments.
The periods of oscillations and phase shifts are determined for the central parts of the filaments. They differ from theoretical predictions for gravitational instability mode.
There could probably be additional factors which influence parameters of oscillations (e.g. MHD transverse wave, Liu et al. 2019).

Turbulence S242 and other regions

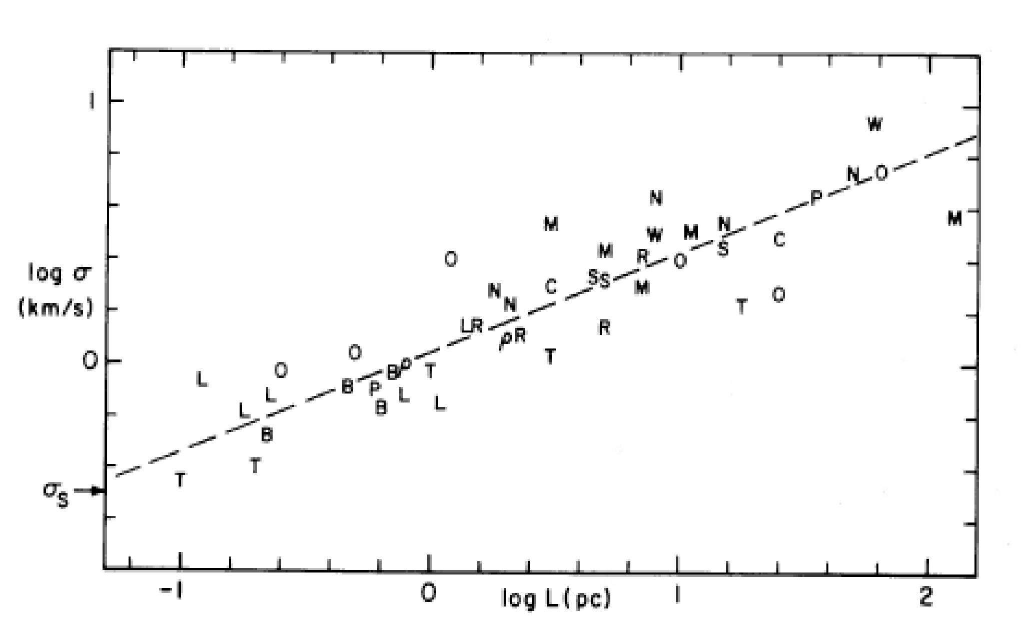

Larson (1981)

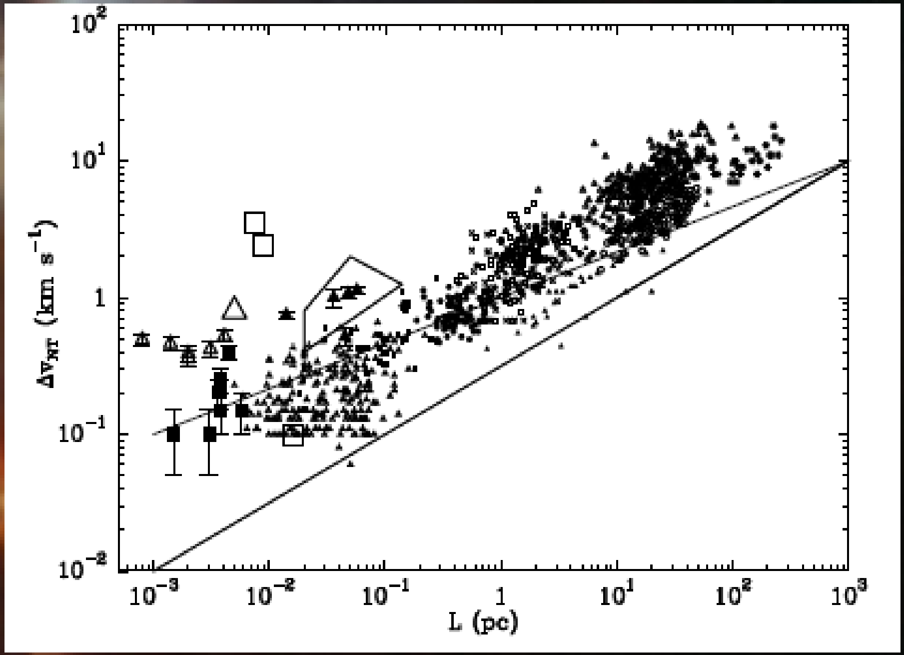

Falgarone et al. (2009)

Velocity structure function

$$S_2(L)^{1/2} = \delta V = \left\langle |V_{\mathrm{lsr}}(r) - V_{\mathrm{lsr}}(r+L)|^2 \right\rangle^{1/2} = v_0\, L^{\gamma}$$

Heyer & Brunt (2004)

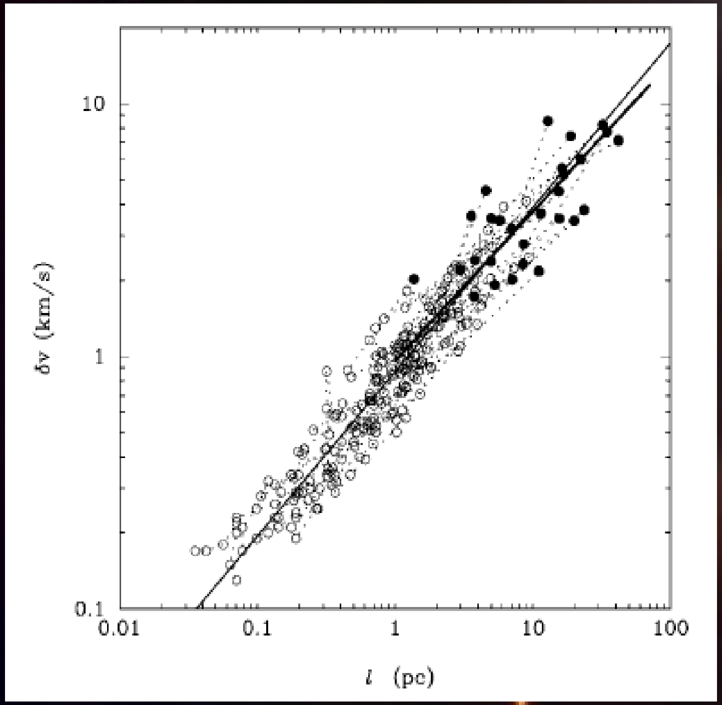

Hacar et al. (2016)

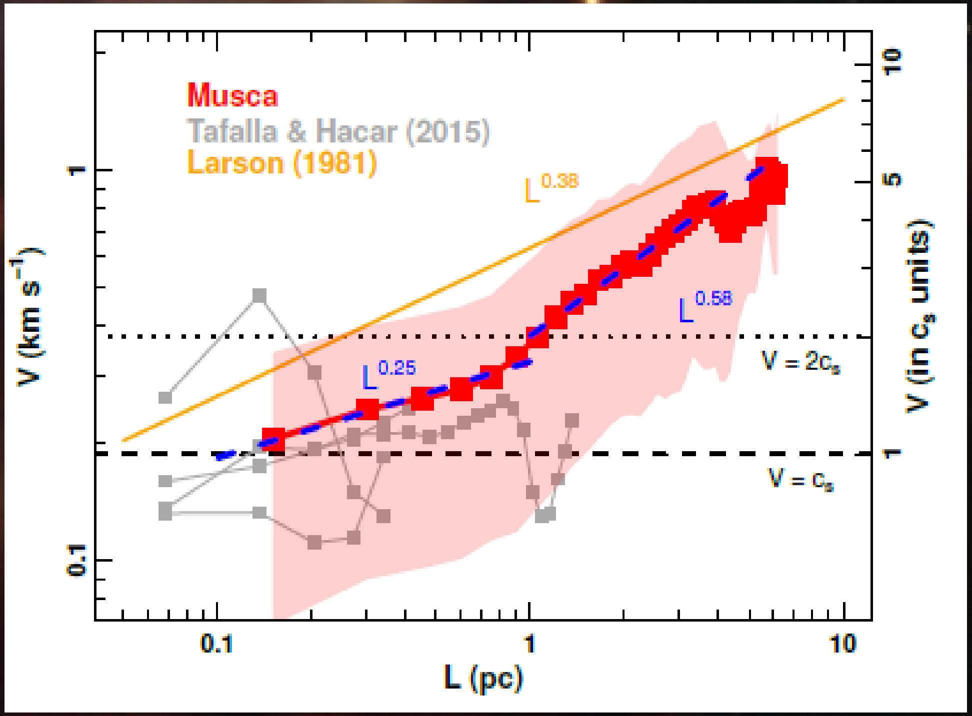

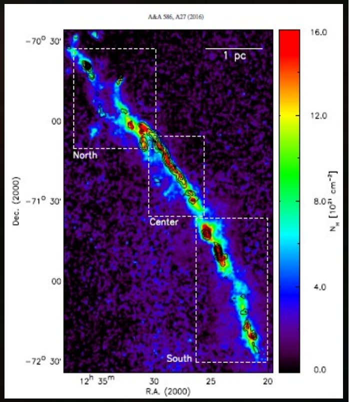

Velocity structure function for S242

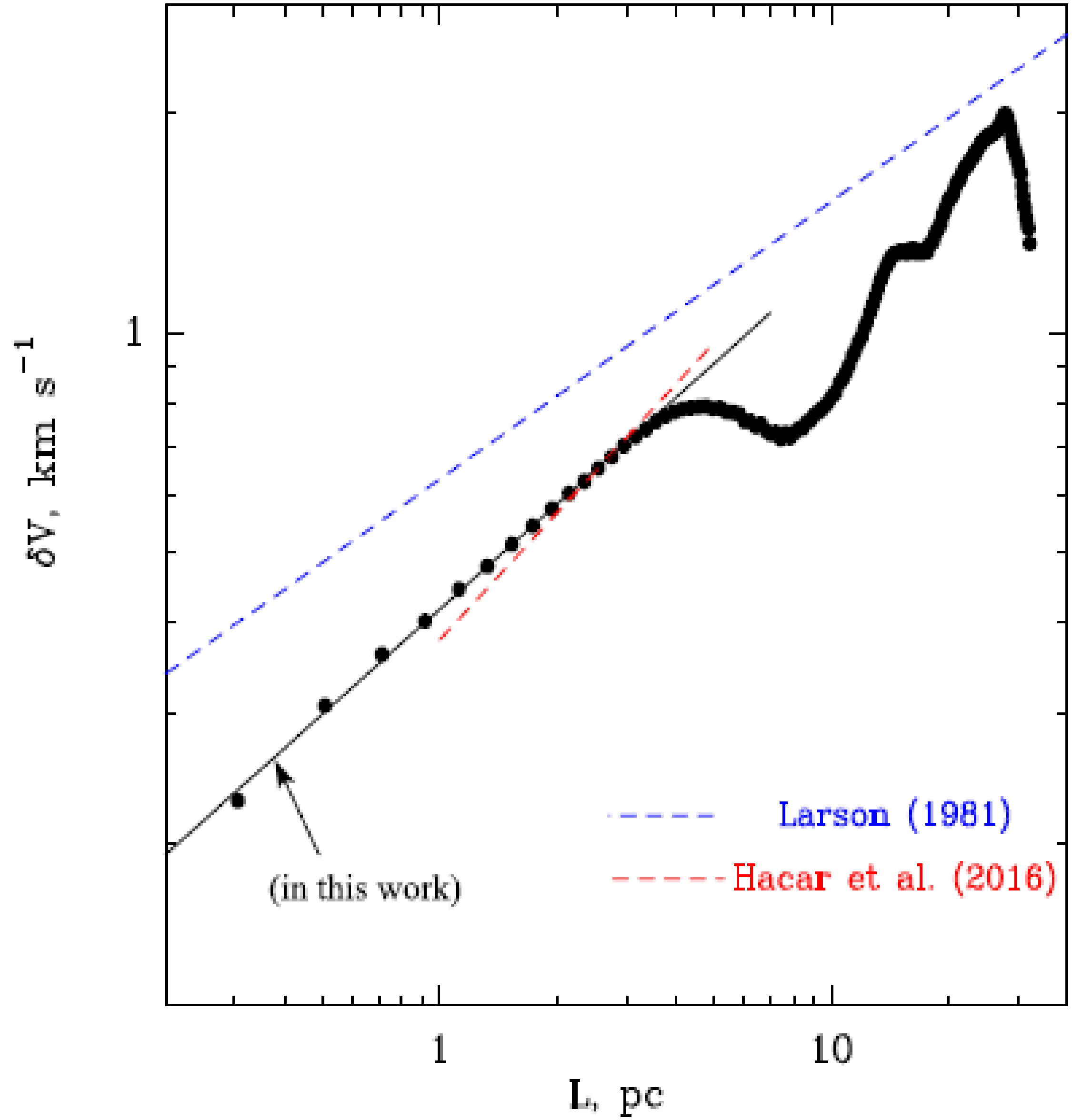

Figure 11. Structure function in velocity δV as a function of length (i.e., lag) derived from the ^{13}CO line data. The structure function is derived using the total data set. The Larson's velocity dispersion–size relationship (i.e., $\delta V = 0.63 \times L^{0.38}$) is also marked by a broken blue line. The velocity dispersion–size relationship of the Musca cloud is also shown by a broken red line (e.g., $\delta V = 0.38 \times L^{0.58}$; Hacar et al. 2016). In the filament, a linear relation is found between $\log(\delta V)$ and $\log(L)$ for $L \lesssim 3$ pc, where $\delta V = 0.42 \times L^{0.48}$ (see the solid black line in the figure as well as the text

$\delta V = 0.42\ L^{0.48}$ (L< ~3 pc)

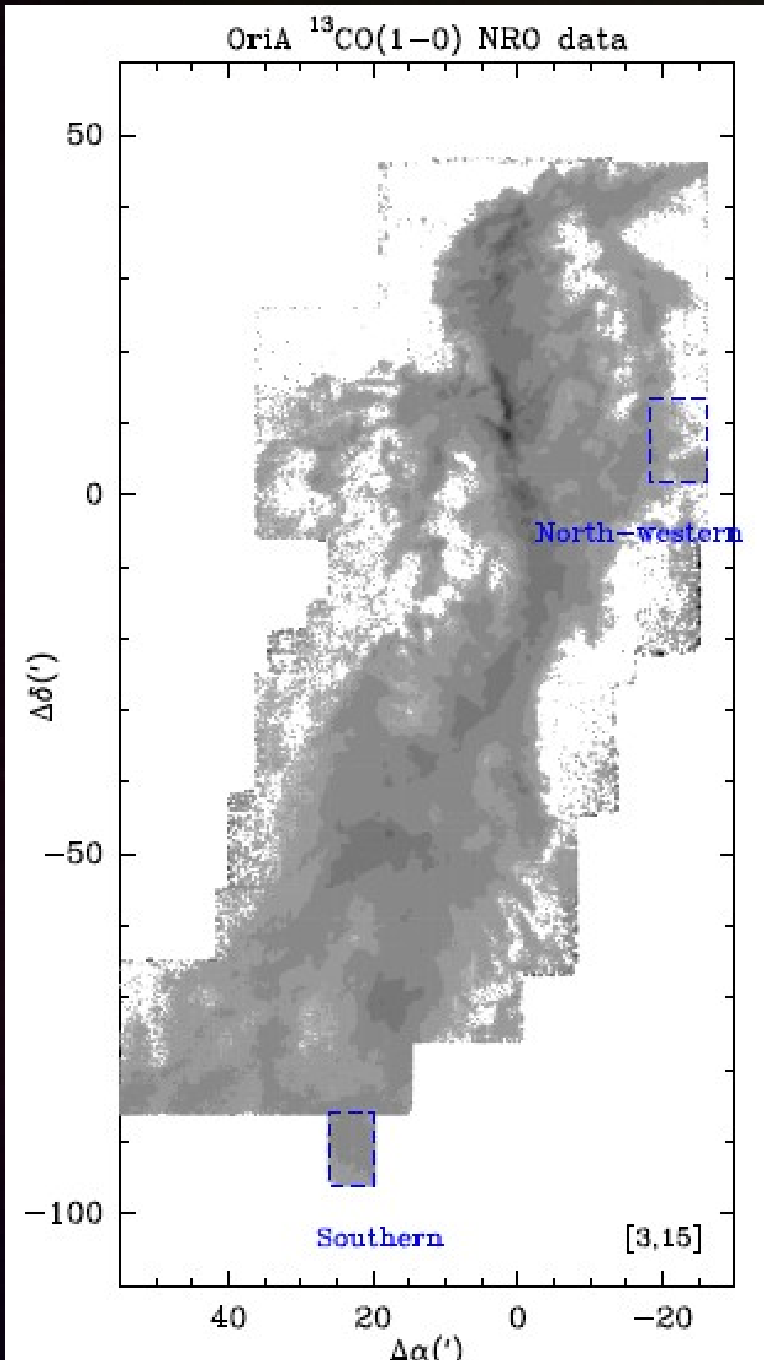

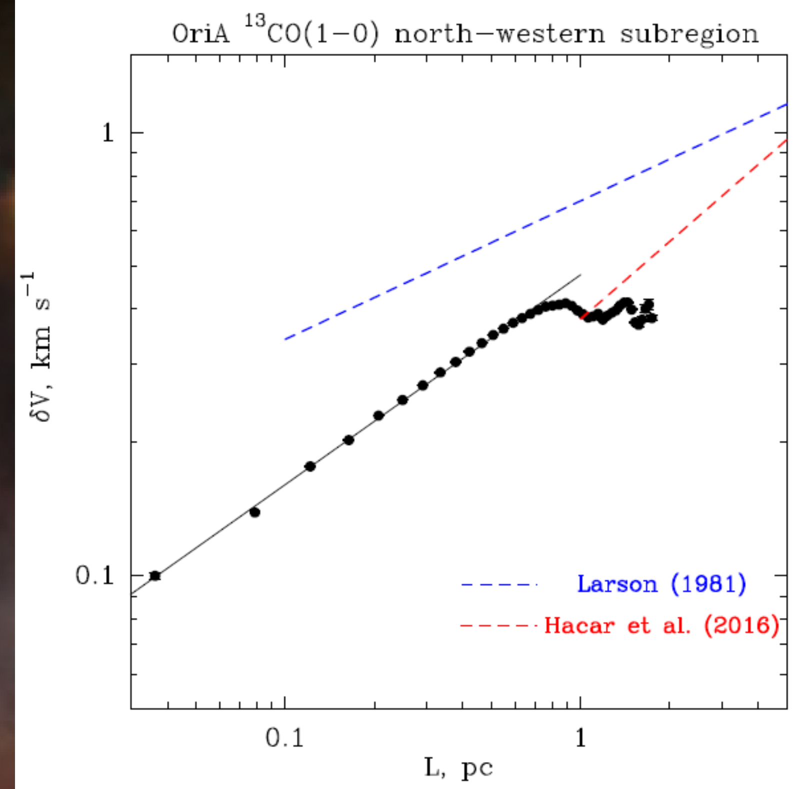

$$\delta V = 0.49\ L^{0.47}$$

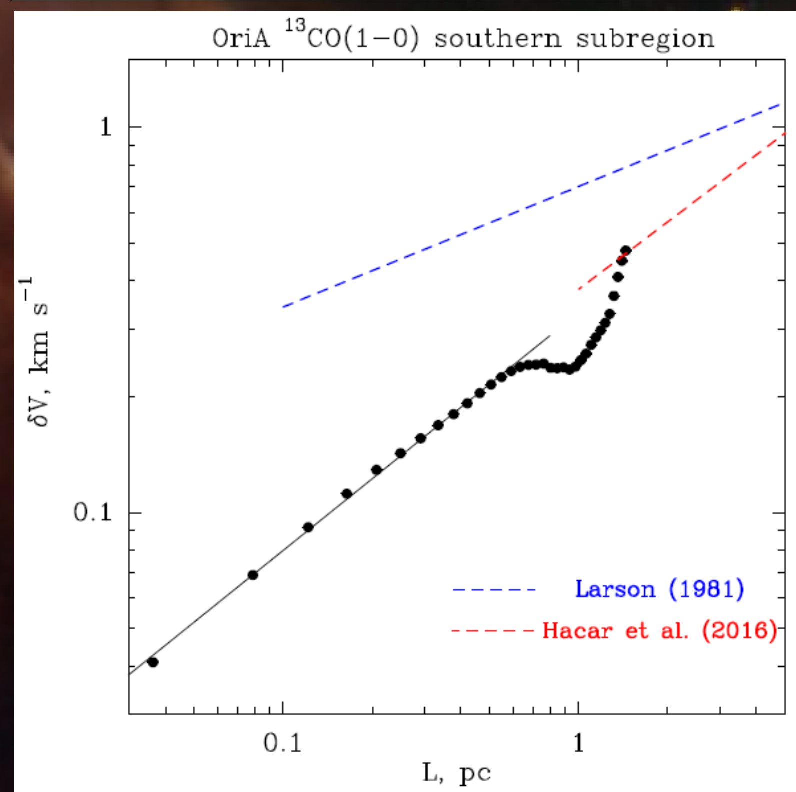

$$\delta V = 0.35\ L^{0.63}$$

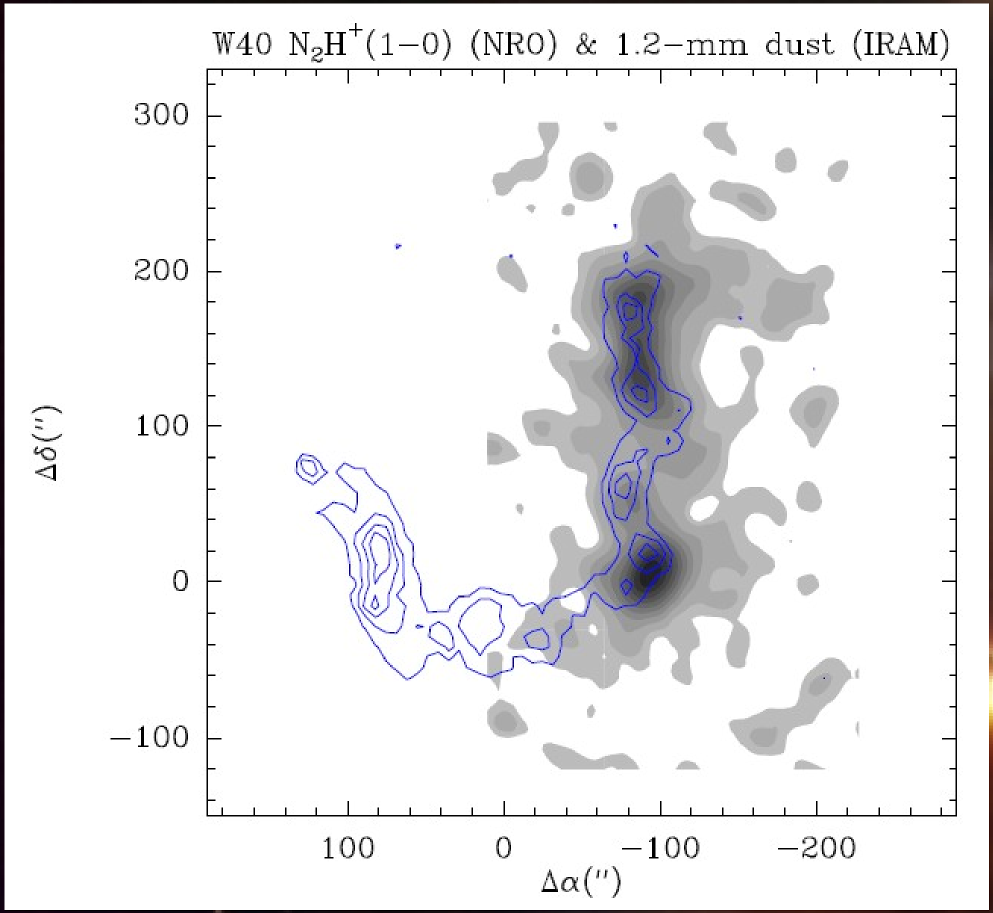

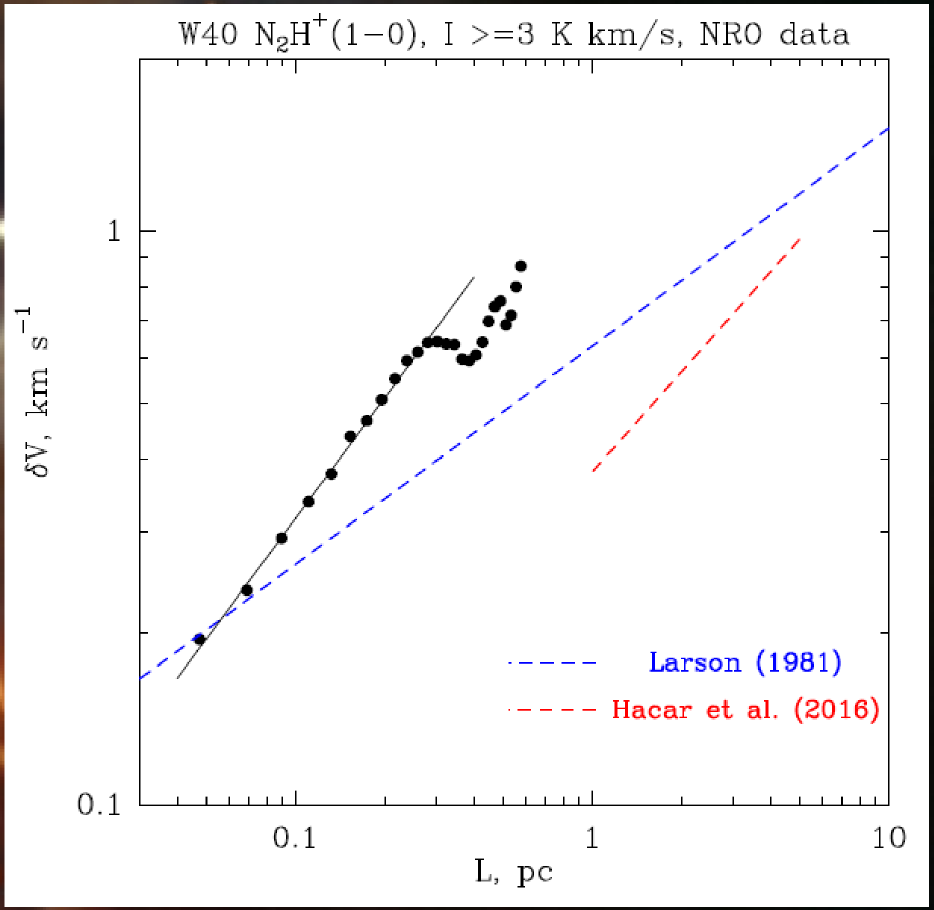

$$\delta V = 0.2\ L^{0.7}$$

An analysis with velocity structure function reveals power-law dependences for S242 and other regions that could be associated with a general behavior of the velocity field on small scales.

It could be a result of the supersonic vortices produced by gas flows along the filament, which dominate at lower lags, or small-scale systematic motions.

An upper scale for a power-law dependence in the S242 filament is ~3 pc, ~0.6-0.7 pc for the Ori A subregions and ~0.2 pc for the W40 region.
The differences in power-law indices could be connected with different levels of turbulent vortices and small-scale systematic motions.

At higher lags contributions from large-scale and ordered velocity gradients and/or filament fragmentation dominate.

Kinematics of the L1287 core from fitting model molecular line maps into observed ones

- The cores are initially quasi-equilibrium (Shu 1977, McKee & Tan 2003), prestellar stage: $V=0$;

- The cores initially are nonequillibrium (Vazquez-Semadeni et al. 2019), prestellar stage: V (envelope) $\sim$ const $\neq 0$

protostellar stage: V (inner region) $\sim 1/\sqrt{r}$

Indications of contraction motions

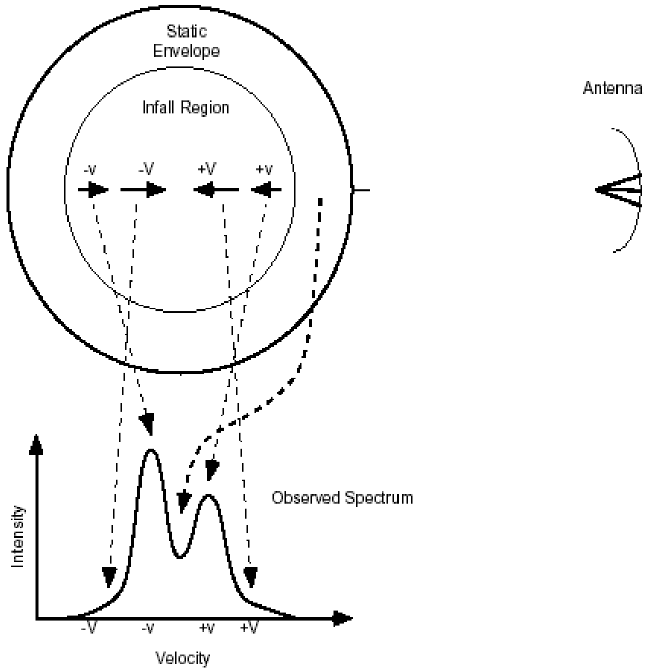

Figure 5: The origin of various parts of the line profile for a cloud undergoing inside-out collapse. The static envelope outside r_{inf} produces the central self-absorption dip, the blue peak comes from the back of the cloud, and the red peak from the front of the cloud. The faster collapse near the center produces line wings, but these are usually confused by outflow wings.

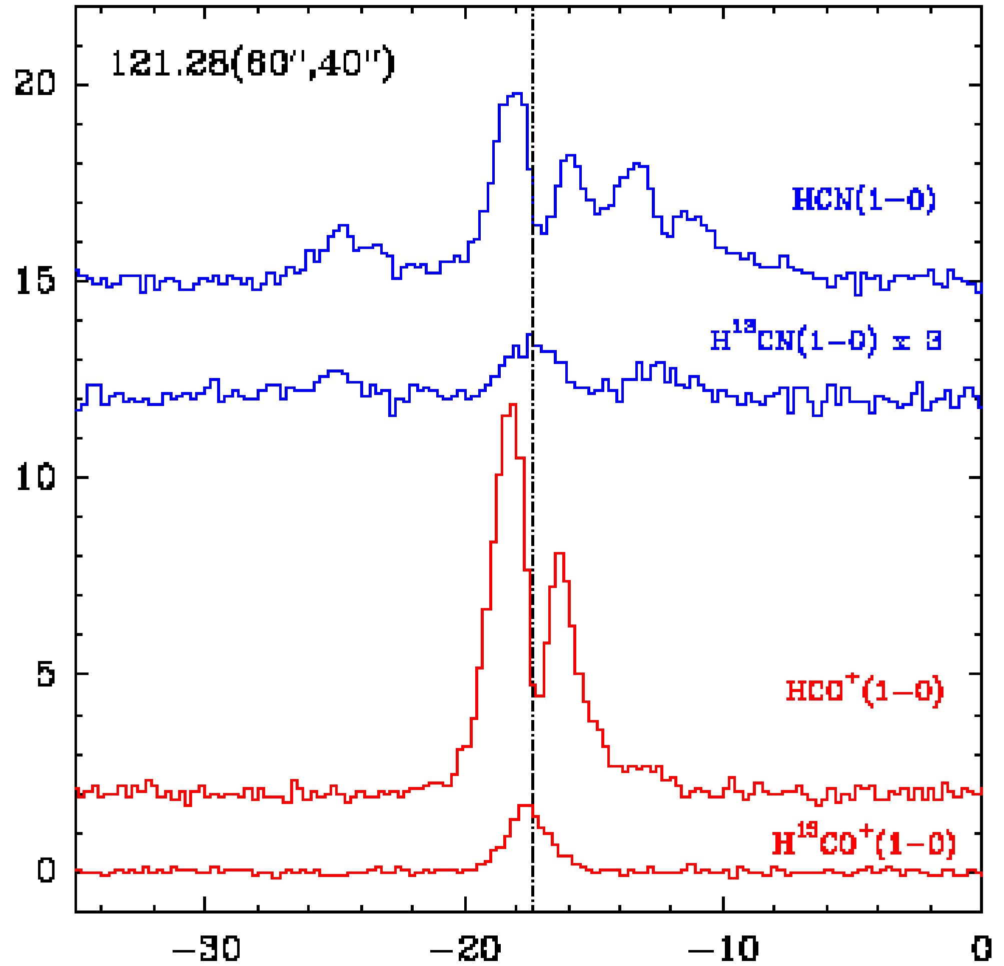

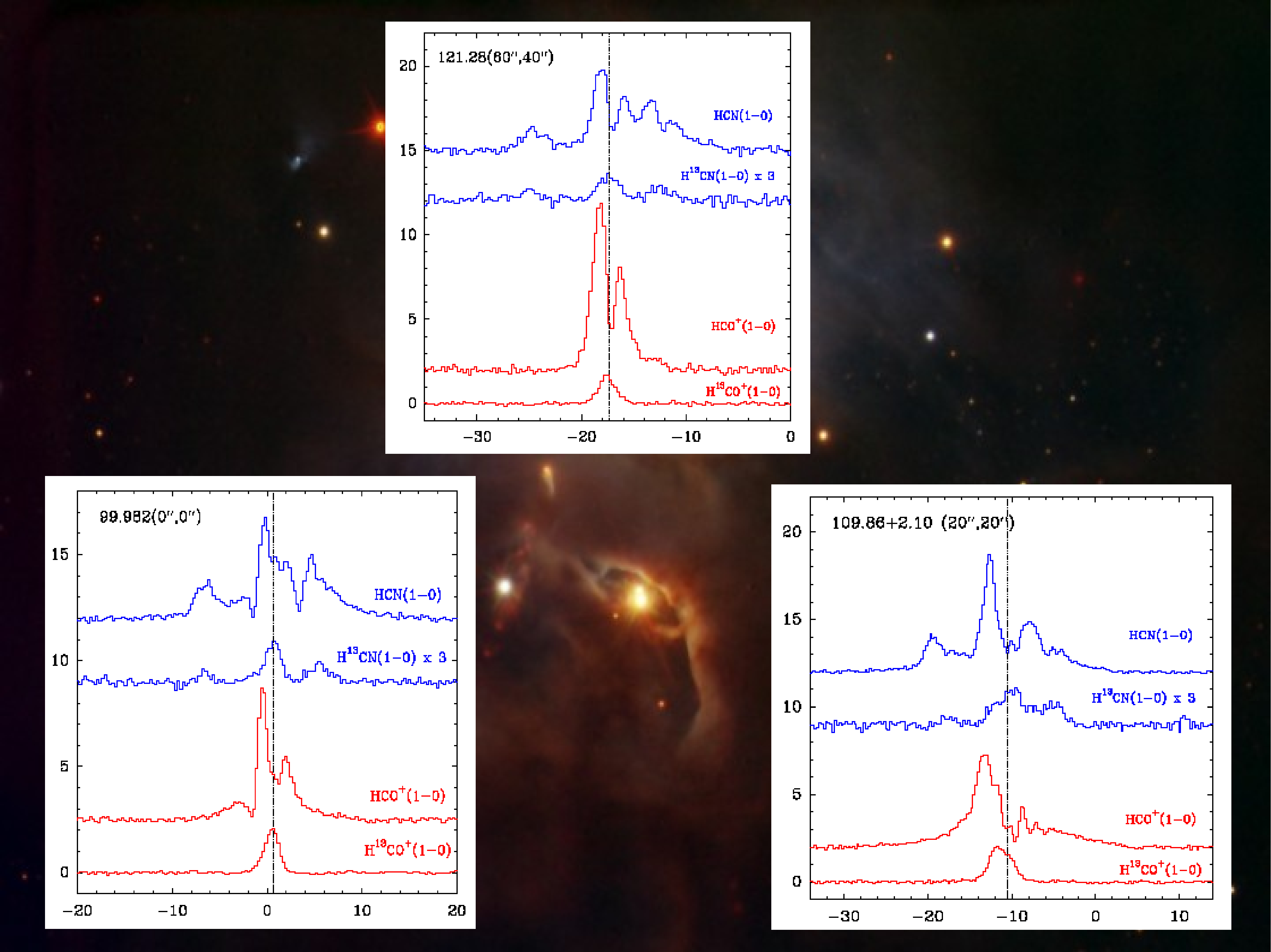

121.28(60″,40″)
HCN(1–0)
H^{13}CN(1–0) x 3
HCO^{+}(1–0)
H^{13}CO^{+}(1–0)
99.982(0″,0″)
HCN(1–0)
H^{13}CN(1–0) x 3
HCO^{+}(1–0)
H^{13}CO^{+}(1–0)
109.86+2.10 (20″,20″)
HCN(1–0)
H^{13}CN(1–0) x 3
HCO^{+}(1–0)
H^{13}CO^{+}(1–0)

L1287 (121.30+0.66)

The Herschel (500 μm, color) and HCO+(3 mm, contours) maps

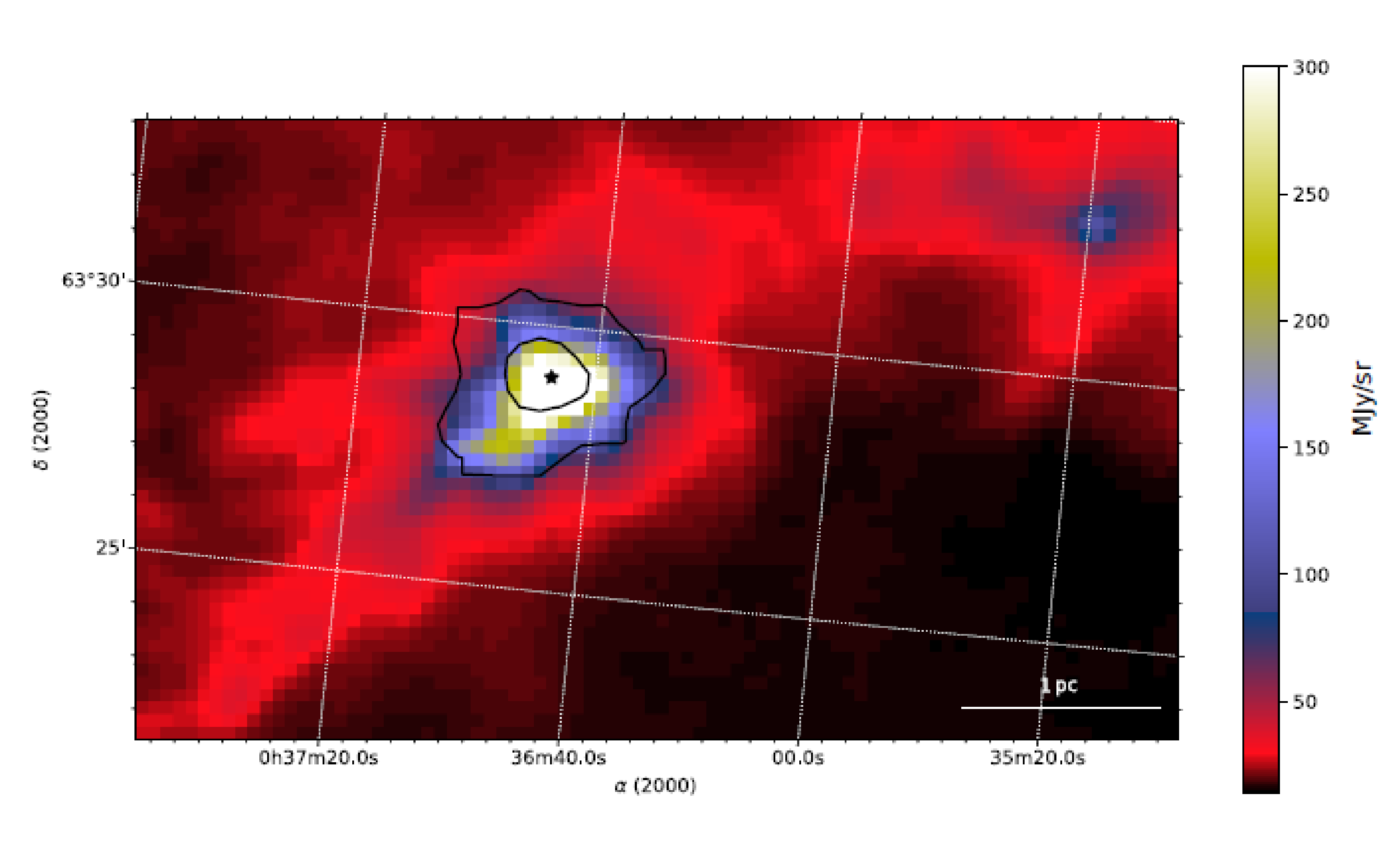

The L1287 core in the HCO+(1-0) and HCN(1-0) lines
(Pirogov et al. 2016)

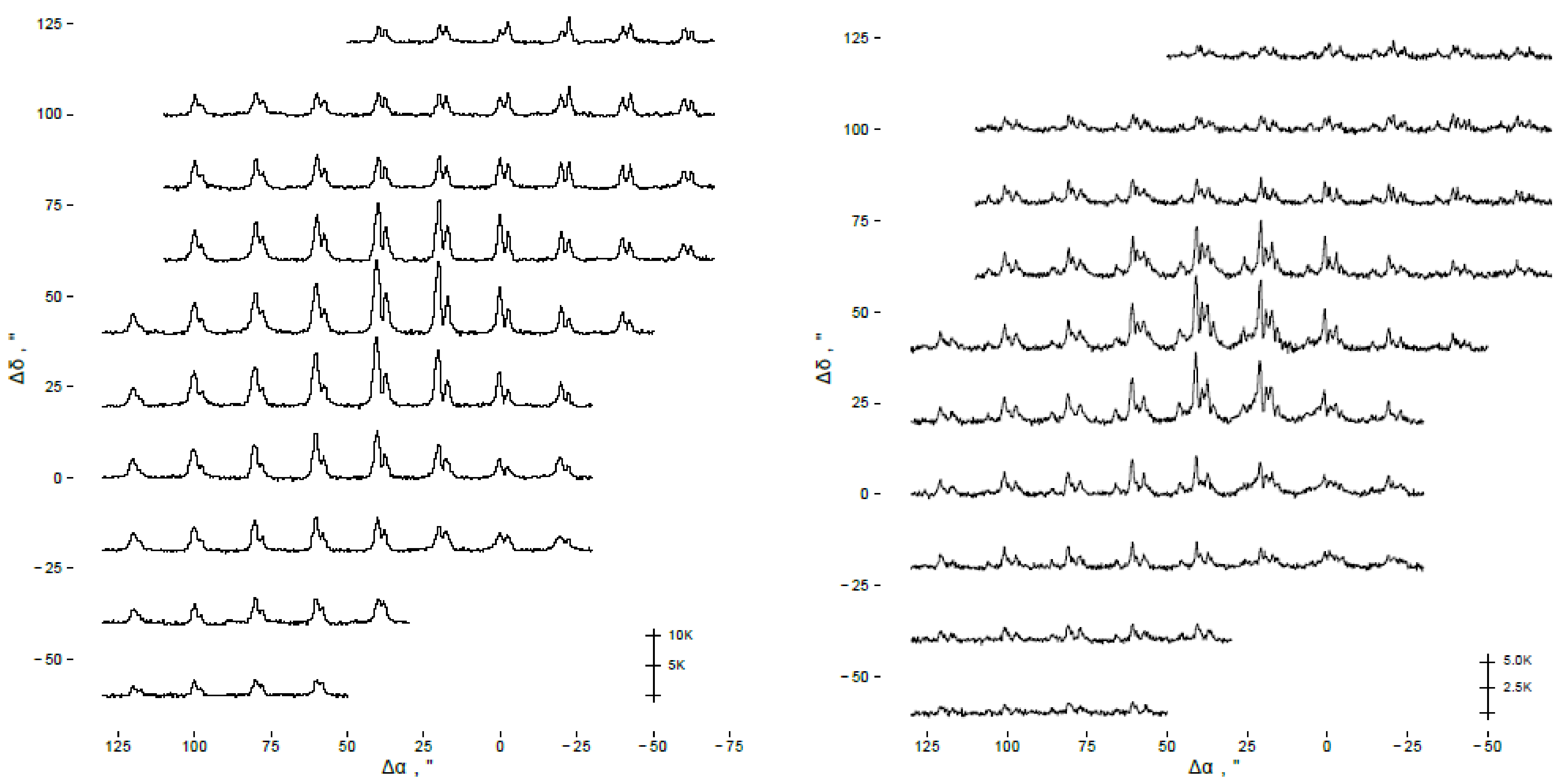

Radial velocity profiles can be derived from fitting model spectral maps into observed ones.

Microturbulent 1D non-LTE model.

Physical parameters (density, temperature, turbulent and systematic motions) depend on radial distance as:

$P = P0/(1+(r/R0)^{\alpha\_p})$

Eight free parameters: P0 & α_p for density, turbulent and systematic velocity radial profiles, molecular abundances (X) and outer radius (R_max). Temperature profile was set to $80/(1+(r/R0)^{0.3})$.

Problems with conventional iterative methods:
multiple minimums of multidimensional error function, correlation between parameters, slow convergence.

The PCA and kNN -based algorithm (Pirogov & Zemlyanukha 2021):

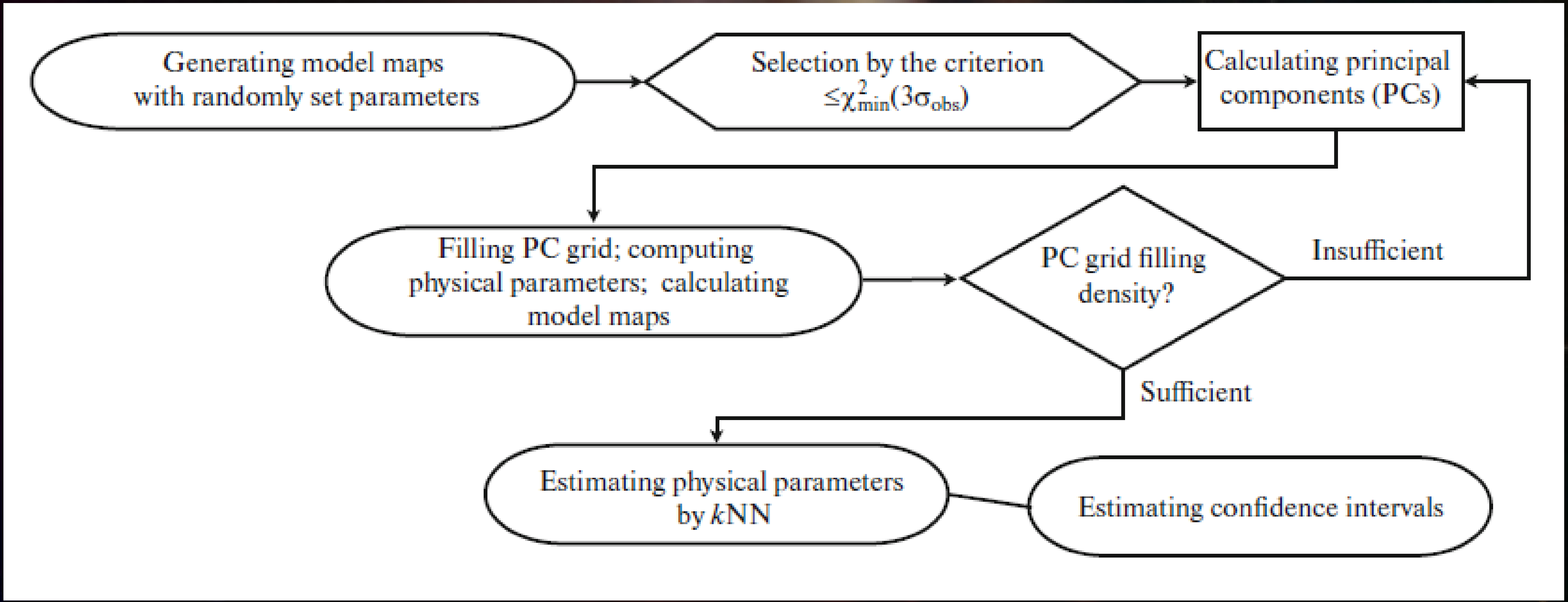

$$\chi^2 = \frac{1}{N_p - n} \sum_{k=1}^{n_{lines}} \sum_{j=1}^{N_k} \sum_{i=1}^{m_k} \frac{(I_{ijk}^{obs} - I_{ijk}^{mod})^2}{\sigma_{jk}^2}$$

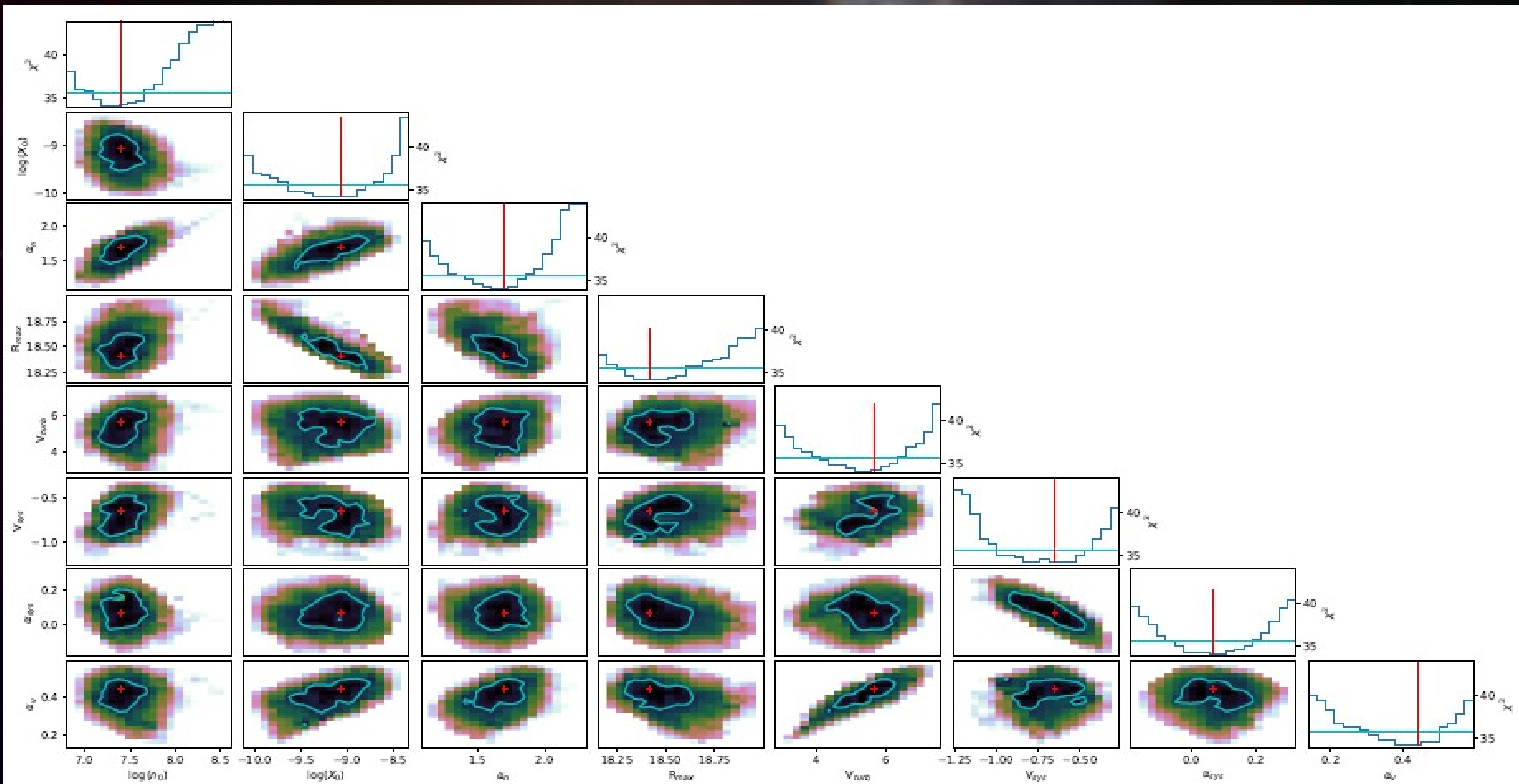

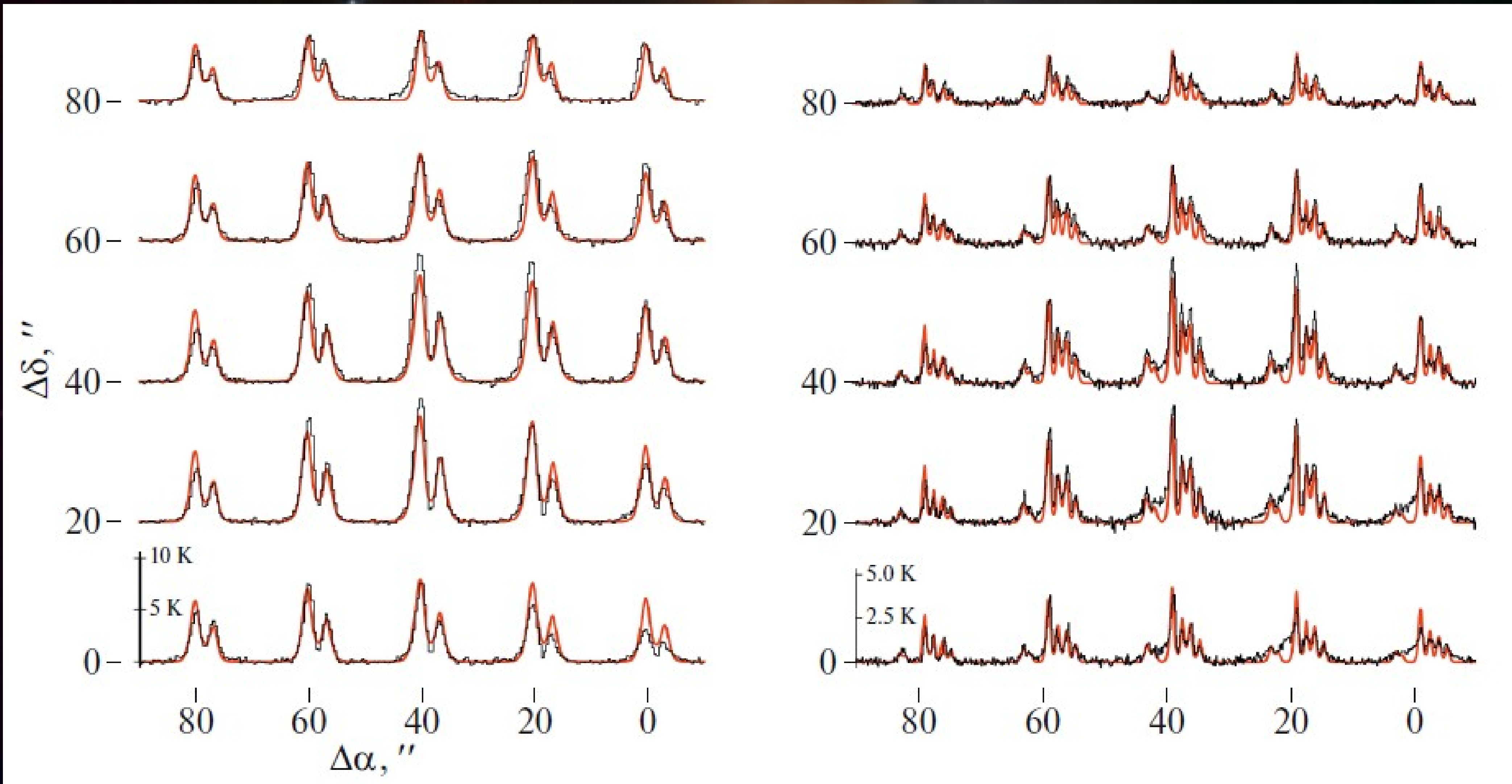

80
60
40
20
0
Δδ, ″
10 K
5 K
80
60
40
20
0
Δα, ″
5.0 K
2.5 K

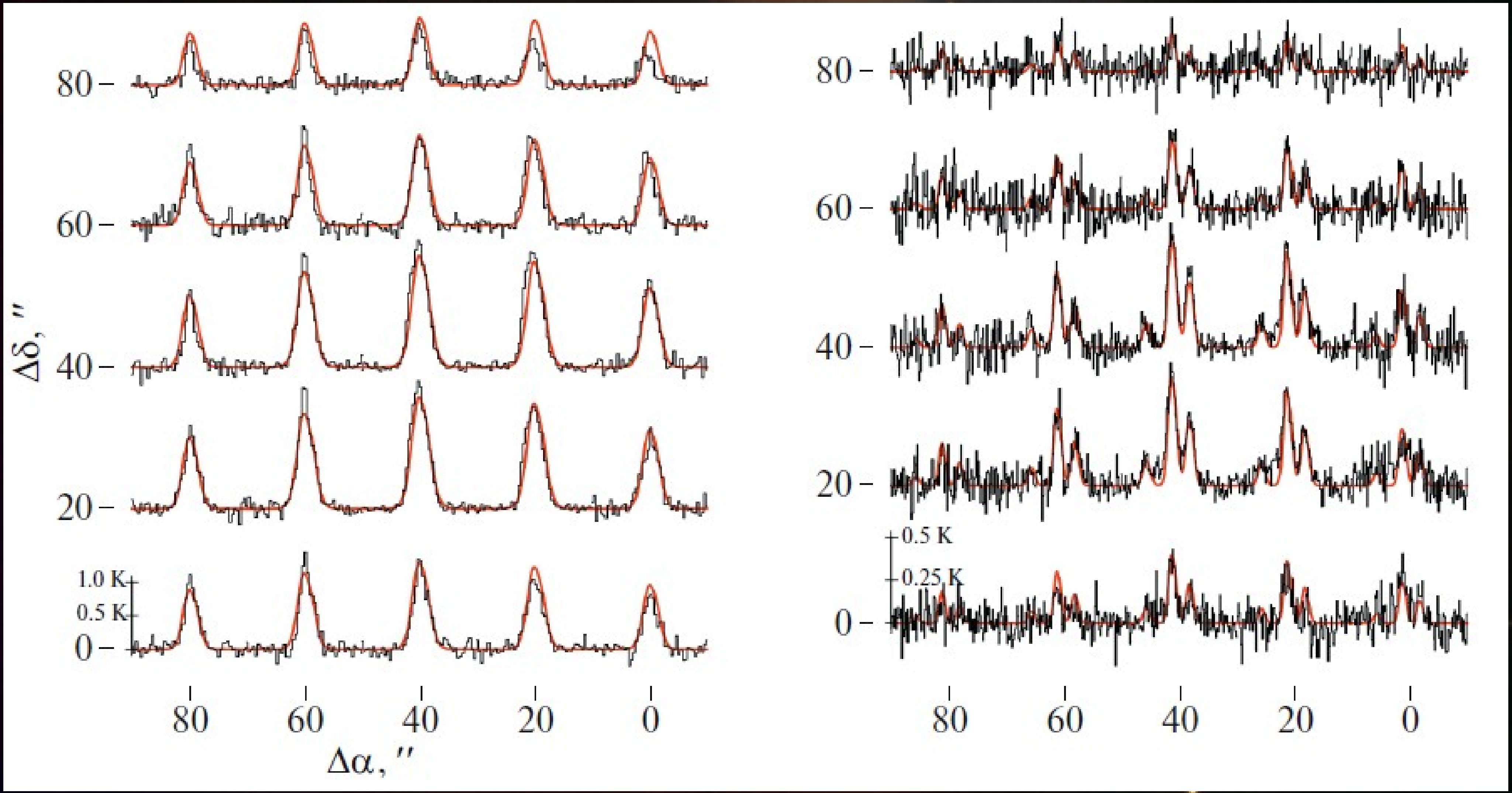

80
60
40
20
0
1.0 K
0.5 K
Δδ, ″
Δα, ″
0.5 K
0.25 K

125
100
75
50
25
0
−25
−50
Δδ , "
Δα , "
10K
5K

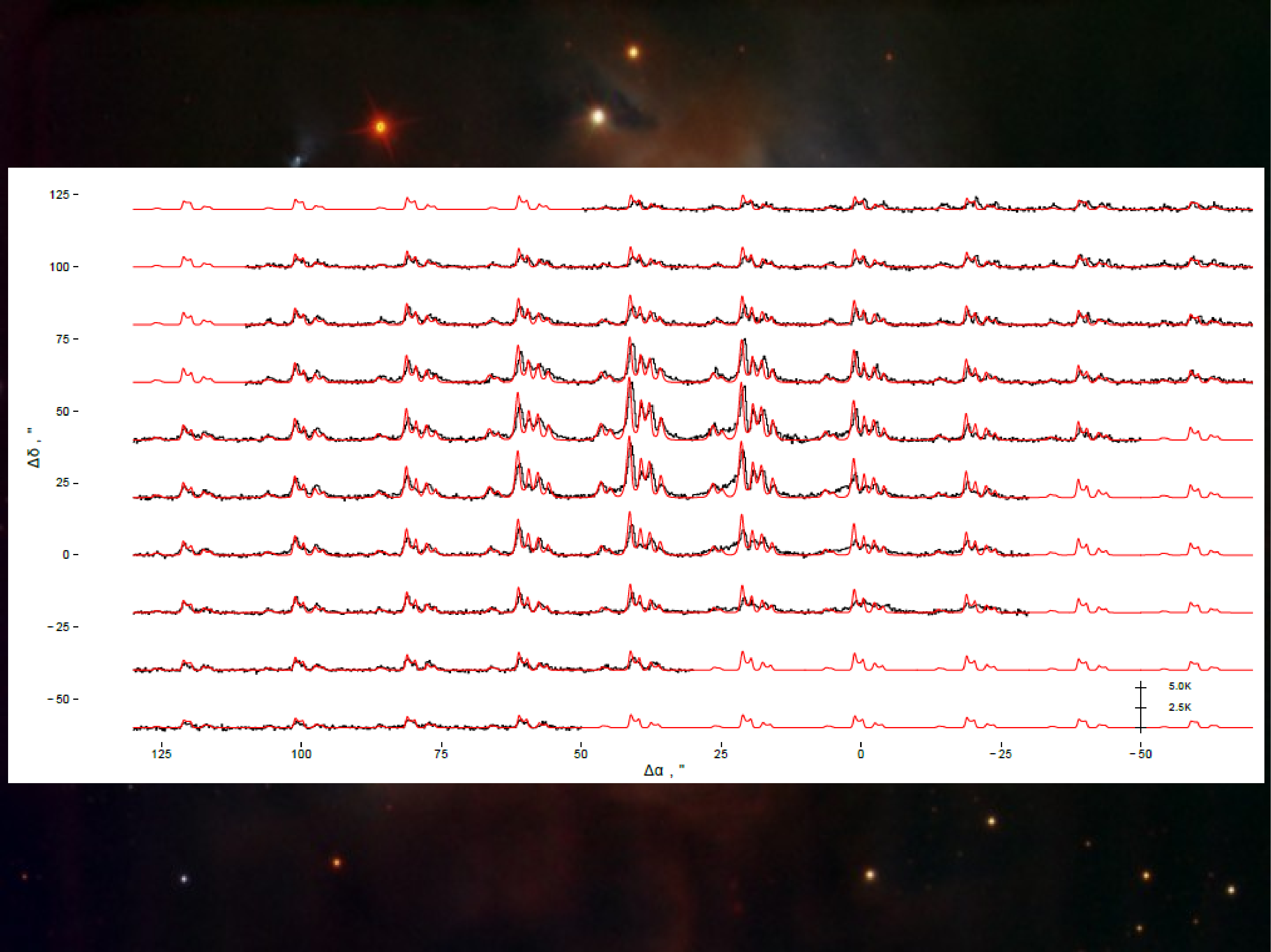
Δδ , "
125
100
75
50
25
0
- 25
- 50
Δα , "
125
100
75
50
25
0
- 25
- 50
5.0K
2.5K

Parameter	Value
$n_0 \times 10^7$, cm^{-3}	$2.6^{+1.7}_{-1.3}$
α_n	$1.7^{+0.1}_{-0.3}$
V_{turb}, km/s	$5.6^{+0.7}_{-1.4}$
α_{turb}	$0.44^{0.05}_{-0.13}$
V_{sys}, km/s	$-0.66^{+0.21}_{-0.24}$
α_{sys}	$0.1^{+0.08}_{-0.13}$
$R_{\max}$, pc	$0.8^{+0.2}_{-0.25}$
$X(HCO^+) \times 10^{-9}$	$1.0^{+0.5}_{-0.4}$
$X(H^{13}CO^+) \times 10^{-11}$	$3.7^{+2.4}_{-2.0}$
$X(HCN) \times 10^{-9}$	$2.5^{+1.4}_{-1.1}$
$X(H^{13}CN) \times 10^{-11}$	$8.5^{+5.3}_{-4.8}$

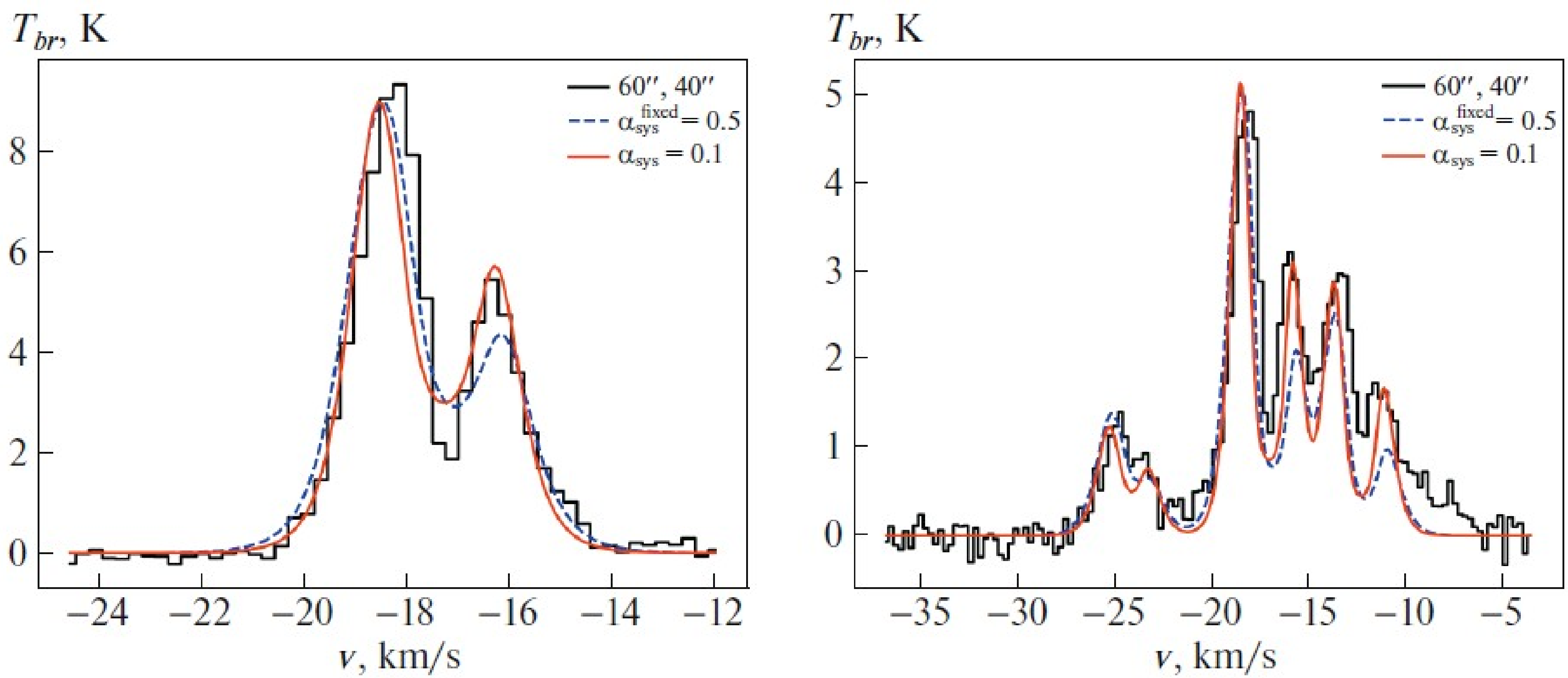

Fig. 8. Observed and model profiles of the lines HCO^+(1–0) (left) and HCN(1–0) (right) towards the (60″, 40″) position for models with different values of the power-law index in the radial profile of contraction velocity.

From fitting of the model HCO+(1–0), HCN(1–0) line maps and line maps of their rare isotopes into the observed maps towards the L1287 core with the PCA and kNN-based algorithm we derived radial profiles of density, turbulent and contraction velocity.

The absolute value of the power-law index for the radial profile of contraction velocity (0.1), considering the probable error, is less than is expected for gas collapse onto the protostar in free fall. This favors the hypothesis that L1287 could be in the mode of global contraction.

Observations of higher molecular transitions as well as the use of more complex non-LTE models (2D, 3D) are needed to confirm this conclusion.


Thanks for your attention!